

Randomized Gradient Descents on Riemannian Manifolds: Almost Sure Convergence to Global Minima in and beyond Quantum Optimization

Emanuel Malvetti^{1,2}, Christian Arenz³, Gunther Dirr⁴,
Thomas Schulte-Herbrüggen^{1,2}

¹School of Natural Sciences, Technische Universität München, Garching, 85748, Germany.

²Munich Center for Quantum Science and Technology (MCQST) & Munich Quantum Valley (MQV), München, 80799, Germany.

³School of Electrical, Computer and Energy Engineering, Arizona State University, Tempe, 85287, Arizona, USA.

⁴Institute of Mathematics, University of Würzburg, Würzburg, 97074, Germany.

Contributing authors: emanuel.malvetti@tum.de;
christian.arenz@asu.edu; dirr@mathematik.uni-wuerzburg.de;
tosh@tum.de;

Abstract

We analyze convergence of gradient-descent methods on Riemannian manifolds. In particular, we study randomization of Riemannian gradient algorithms for minimizing smooth cost functions (of Morse–Bott type). We prove that randomized gradient descent methods, where the Riemannian gradient is replaced by a random projection of it, converge to a single local optimum almost surely despite the existence of saddle points. We consider both uniformly distributed and discrete random projections. We also discuss the time required to pass a saddle point. As a major application, we consider ground-state preparation through quantum optimization over the unitary group. In mathematical terms our randomized algorithm applied to the trace function $U \rightarrow \text{tr}(AU\rho U^*)$ almost surely converges to its *global minimum*. The minimum corresponds to the smallest eigenvalue (ground state) of the selfadjoint operator A (Hamiltonian) if ρ is a rank-one projector (pure state). In this setting, one can efficiently replace the uniform random projections by implementing so-called discrete unitary 2-designs.

Keywords: Riemannian gradient system, randomized gradient descent, Morse–Bott systems, saddle-point escape, quantum optimization

MSC Classification: 65K10 , 53B21 , 37H10

1 Introduction

Both gradient systems and numerical linear algebra come with a long history, as well as a vibrant research activity. For instance, gradient systems have been advanced lately from Hilbert manifolds [Neuberger \(2010\)](#) to general metric spaces (e.g., in the context of optimal mass transport [Ambrosio et al \(2021\)](#); [Mielke \(2023\)](#)). In contrast, numerical linear algebra has faced factorization problems of large tensor structures [Batselier et al \(2018\)](#) (tensor SVD) using “randomization strategies” for their classical algorithms in order to handle these huge amounts of data. A few decades ago, a systematic study of their interplay started by analyzing the QR-algorithm and interior point methods from a (Riemannian) geometric point of view, cf. the collection of [Bloch \(1994\)](#). In this development, the seminal work of [Brockett \(1988, 1989\)](#) on the so-called “double-bracket flow” on orbits of the orthogonal group (and likewise of the unitary group in [Brockett \(1993\)](#)), followed by independent similar ideas of [Chu and Driessel \(1990\)](#), has sparked a plethora of applications. For an early overview on optimization techniques on Riemannian manifolds (including higher-order methods) see [Smith \(1994\)](#) and [Bloch \(1994\)](#). A detailed mathematical account can be found in the monograph by [Helmke and Moore \(1994\)](#), including discretization schemes, suitable step sizes, and proofs of convergence. For the latter, the authors heavily exploited the Morse–Bott structure of the respective cost functions (i.e. the particular structure of the Hessian at possibly non-isolated critical points, cf. Subsec. 2.3 here and [Duistermaat et al \(1983\)](#)) to obtain convergence to a single critical point. Based on these developments, higher-order methods with applications to a variety of cost functions on classical matrix manifolds are treated in [Absil et al \(2008\)](#) or, more recently, by [Boumal \(2023\)](#). In [Schulte-Herbrüggen et al \(2010\)](#), the above ideas have been extended to flows and their discretization schemes on more general homogeneous spaces. There, the authors also established connections to applications in quantum dynamics as well as to applications in numerical (multi-)linear algebra, such as higher-rank tensor approximations — as elaborated by [Curtef et al \(2012\)](#) to complement standard methods (such as higher-order powers of [de Lathauwer et al \(2000\)](#) or quasi-Newton methods of [Savas and Lim \(2010\)](#)).

Independently, in the physics community, [Wegner \(1994\)](#) (re)devised gradient flows of Brockett type, e.g., to (band-)diagonalize Hamiltonians, which the monograph by [Kehrein \(2006\)](#) elaborated to address further quantum many-body applications.

Often, gradient-flow approaches for deriving optimization schemes on Riemannian manifolds hinge on the computability of the Riemannian exponential, ensuring to take the gradient from the tangent space back to the manifold. To be precise, this is crucial whenever the manifold cannot be identified with its tangent spaces, such as for the

unitary group and its orbits. But, in particular in this case, analytical expressions and efficient numerical approximations for the Riemannian exponential are well known.

With these stipulations, Riemannian optimization constitutes a versatile toolbox, since cost functions can readily be tailored to the particular application such as finding extremal eigen- or singular values. These instances also connect to other branches of mathematics such as numerical and C -numerical ranges and their extremal values, the numerical and C -numerical radii (see [Gustafson and Rao \(1997\)](#); [Li \(1994\)](#)).

Over the last decade, techniques from Riemannian optimization have also been adopted in quantum information science. For example, in quantum computing, hybrid quantum-classical algorithms [Bharti et al \(2022\)](#), such as variational quantum algorithms (VQAs) [Cerezo et al \(2021\)](#); [Tilly et al \(2022\)](#), have been developed to solve ground-state problems [Peruzzo et al \(2014\)](#), combinatorial optimization problems [Farhi et al \(2014\)](#), and quantum machine learning problems [Biamonte et al \(2017\)](#). [Wiersema and Killoran \(2023\)](#) proposed projecting the Riemannian gradient into smaller dimensional subspaces to obtain scalable¹ quantum-computer implementations. However, the “dimension reduction” strategy comes at a cost: While the full gradient flow converges almost surely to some local minimum in spite of strict saddle points² [Lee et al \(2019\)](#), for the projected versions no such guarantees can be made. Indeed, numerical simulations see convergence to artificial local minima induced by the projection into a *fixed* subspace. Inspired by the success of classical randomized gradient descent [Ruder \(2016\)](#), the problem of artificial minima has recently been circumvented by some of the authors in [Magann et al \(2023\)](#) via “random projections” of the Riemannian gradient. (Details on different optimization algorithms and their efficient implementations on *quantum* computers are postponed to Section 5.)

In this paper we consider the randomized gradient algorithm presented in [Magann et al \(2023\)](#) in the more general setting of the large class³ of Morse–Bott cost functions on Riemannian manifolds. For both continuous and discrete probability distributions of the random gradient directions, we prove that in fact the algorithm almost surely converges to a local minimum. This is a significant improvement on the state-of-the-art, where thus far (see [Gutman and Ho-Nguyen \(2023\)](#)) only convergence to the *set* of critical points has been proven without the Morse–Bott assumption. Related papers have established convergence to local optima for perturbed and stochastic gradient descent [Jin et al \(2021\)](#), also generalized to Riemannian manifolds [Criscitiello and Boumal \(2019\)](#) and [Sun et al \(2019\)](#). Finally, we show how our result can be applied to quantum optimization tasks, such as ground state preparation: It is by construction that in the specific quantum setting, there are no local optima, whereby we prove that our randomized gradient algorithm then converges almost surely to a single *global* minimum.

¹Sec. 5 gives a precise meaning of ‘scalable quantum computers’

²i.e., saddle points at which the Hessian has at least one negative eigenvalue

³Indeed, on a compact manifold, the set of Morse functions, which is a subset of the Morse–Bott functions, forms an open dense subset of the space of smooth functions [Audin \(2014\)](#). In this sense, Morse–Bott functions are generic.

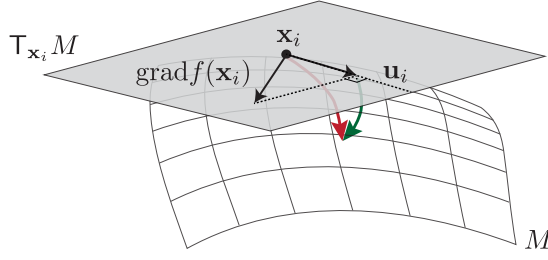


Fig. 1 Schematic representation of a randomized gradient descent algorithm on a Riemannian manifold M . At a point \mathbf{x}_i on M , the Riemannian gradient $\text{grad } f(\mathbf{x}_i)$ of a cost function $f : M \rightarrow \mathbb{R}$ lies in the tangent space $T_{\mathbf{x}_i}M$ depicted as the plane spanned by \mathbf{u}_i and its orthocomplement. Instead of iteratively following the full gradient in order to optimize f , here in each step we consider a projection of $\text{grad } f(\mathbf{x}_i)$ onto a randomly chosen tangent-space direction \mathbf{u}_i . This is key for *efficient* implementations of gradient flows in large-scale quantum optimization problems. In the case of the special unitary group the randomized directions are given by (traceless) skew-Hermitian operators $\mathbf{u}_i = iH_i$. The corresponding quantum circuit consists of a sequence of unitary transformations as shown in Fig. 5, where the cost function is then denoted by J .

Structure and Main Results

In Sec. 2 we introduce the fundamental notions from Riemannian geometry to describe gradient flows (Sec. 2.1), recollecting some well-known results on the convergence of such gradient flows (Secs. 2.2 and 2.3), and their algorithmic implementation as gradient descents (Sec. 2.4). In Sec. 3 we describe a gradient descent algorithm where, in each step, the full gradient of a high-dimensional problem is projected on just a randomly chosen direction of the tangent space as illustrated in Fig. 1. We consider both uniformly distributed⁴ and discrete random directions.

The main results are obtained in Secs. 3.2 and 3.3, where we prove that a randomly projected gradient descent algorithm of a smooth Morse–Bott cost function (with compact sublevel sets) on a Riemannian manifold comes with two vitally beneficial properties: (i) *it almost surely escapes saddle points* — as is shown in Lem. 3.14, and as a consequence (ii) *it almost surely converges to a single local minimum* — as shown in Thm. 3.17.

In Sec. 4, the case of a two-dimensional saddle point is studied using analytical methods and numerical simulation. We obtain good approximations for the time necessary to pass the saddle point.

Finally, Sec. 5 shows how the previous results can be applied in quantum optimization: by construction, the important problem class of ground-state preparation comes with the particular advantage that our algorithm achieves almost sure convergence to a single *global* minimum. Moreover, in these cases the algorithm can be efficiently implemented on quantum computers.

⁴with respect to the Haar measure

2 Riemannian Gradient Flow and Descent

2.1 Basic Concepts

First, we recall some basic notions and notations from Riemannian geometry. Let M denote a finite dimensional smooth manifold of dimension N with tangent and cotangent bundles TM and T^*M , respectively. Moreover, let M be endowed with a Riemannian metric \mathbf{g} , i.e. a smoothly varying scalar product $\mathbf{g}(\mathbf{x}) = \langle \cdot, \cdot \rangle_{\mathbf{x}}$ on each tangent space $T_{\mathbf{x}}M$, $\mathbf{x} \in M$. The pair (M, \mathbf{g}) is called a *Riemannian manifold*. For ease of notation we will usually omit the subscript in the scalar product and write $\langle \cdot, \cdot \rangle$ and similarly $\| \cdot \|$ for the resulting norm.

Every Riemannian manifold is equipped with a Riemannian density μ induced by the metric \mathbf{g} , see (Lee, 2013, Prop. 2.44). This density can be used to integrate functions, to induce a measure on M and to define sets of measure zero. Equivalently (but without introduction of a Riemannian density), one could say that $S \subset M$ has measure zero if there is an atlas such that $S \cap \text{dom } \sigma$ has Lebesgue measure zero in every chart σ . In particular, any submanifold of dimension strictly smaller than N has measure zero.

2.2 Gradient Flows and Asymptotic Behaviour (I)

In the following general description, we depart from the above notation of ‘the’ cost function J borrowed from quantum optimization and introduce $f : M \rightarrow \mathbb{R}$ for an arbitrary smooth (cost) function on M with differential $df : M \rightarrow T^*M$. Then the gradient of f at $\mathbf{x} \in M$, denoted by $\text{grad } f(\mathbf{x})$, is the unique vector in $T_{\mathbf{x}}M$ determined by the identity

$$df(\mathbf{x})\xi = \langle \text{grad } f(\mathbf{x}), \xi \rangle \quad (1)$$

for all $\xi \in T_{\mathbf{x}}M$. Equation (1) naturally defines a vector field on M via $\text{grad } f : M \rightarrow TM$, $\mathbf{x} \rightarrow \text{grad } f(\mathbf{x})$ called gradient vector field of f . The corresponding ordinary differential equation

$$\dot{\mathbf{x}} = -\text{grad } f(\mathbf{x}) =: F(\mathbf{x}) \quad (2)$$

and its flow are referred to as the *gradient system* and the *gradient flow* of f , respectively.

In local coordinates, the above reads as follows: Let $\sigma : U \rightarrow \mathbb{R}^N$ be a chart about $\mathbf{x} \in M$, denote $\mathbf{y} = \sigma(\mathbf{x})$, and let $\tilde{f} := f \circ \sigma^{-1}$ be the chart representation of f . Moreover, let $\tilde{\mathbf{g}} := \sigma_* \mathbf{g}$ be the chart representation (where σ_* denotes the pushforward) of the metric \mathbf{g} on $\sigma(U)$, i.e. $\tilde{\mathbf{g}}(\mathbf{y}) = \sum_{i,j=1}^n \tilde{g}_{ij}(\mathbf{y}) dy^i dy^j$, where $\tilde{G}(\mathbf{y}) := (\tilde{g}_{ij}(\mathbf{y}))$ is a positive definite matrix varying smoothly in $\mathbf{y} \in \sigma(U)$. Finally, let $\tilde{F} := \sigma_* F$ be the chart representation of the gradient vector field $-\text{grad } f$. Then it holds that

$$\tilde{F}^j(\mathbf{y}) = - \sum_{i=1}^n \tilde{g}^{ij}(\mathbf{y}) \frac{\partial \tilde{f}}{\partial y_i}(\mathbf{y}),$$

where $\tilde{g}^{ij}(\mathbf{y})$ are the entries of the inverse of $\tilde{G}(\mathbf{y})$ and $\frac{\partial}{\partial y_i}$ denotes the i -th partial derivative.

Any convergence analysis of gradient systems is based on the following two observations: (i) the critical points of f are the equilibria of (2), (ii) f constitutes a Lyapunov function for (2), i.e. f is monotonically decreasing along solutions. Despite their simplicity, they immediately allow several non-trivial statements about the asymptotic behavior of (2), which can be characterized by its ω -limit sets

$$\omega(\mathbf{x}_0) := \bigcap_{s>0} \overline{\{\varphi(t, \mathbf{x}_0) \mid t > s\}},$$

where $t \mapsto \varphi(t, \mathbf{x}_0)$ denotes the unique solution of (2) with initial value $\varphi(0, \mathbf{x}_0) = \mathbf{x}_0$.

Proposition 2.1 (Lee (2013)). *If f has compact sublevel sets, i.e. if the sets $\{\mathbf{x} \in M : f(\mathbf{x}) \leq c\}$ are compact for all $c \in \mathbb{R}$, then every trajectory of (2) converges to the set of critical points. More precisely, every trajectory of (2) exists for all $t \geq 0$ and its ω -limit set is a non-empty, compact and connected subset of the set of critical points of f .*

Although Prop. 2.1 shows that $\omega(\mathbf{x}_0)$ is contained in the set of critical points of f , it does not guarantee convergence to a single critical point and, indeed, there are smooth gradient systems whose trajectories exhibit a non-trivial convergence behavior to the set of critical points (cf. “Mexican hat counter-example” by Curry (1944)). Yet for isolated critical points, one has the following trivial consequence of Prop. 2.1.

Corollary 2.2. *If f has compact sublevel sets and all critical points are isolated, then any solution of (2) converges (for $t \rightarrow \infty$) to a single critical point of f . Moreover, if additionally all saddle points are strict,⁵ then for almost all initial points (in the sense of Sec. 2.1), the flow converges to a local minimum.*

Continua of critical points are much more subtle to handle. Some enhanced conditions guaranteeing convergence to a single critical point will be briefly discussed in the next subsection.

2.3 The Hessian, Morse–Bott Functions and Asymptotic Behaviour (II)

As in the Euclidian case, linearizing the vector field F at its equilibria sheds light on its local stability. Clearly, since $F = -\text{grad } f$ constitutes a gradient vector field, its linearization at an equilibrium $\mathbf{x} \in M$ is given by the Hessian $H_f(\mathbf{x})$ of f at $\mathbf{x} \in M$. In general, if M is non-Euclidian, the computation of $H_f(\mathbf{x})$ can be rather involved. Yet, at critical points $\mathbf{x}_0 \in M$ of f , the *Hessian* is given by the symmetric bilinear form

$$H_f(\mathbf{x}_0)(\xi, \eta) := \sum_{i,j=1}^n \tilde{H}(f \circ \sigma^{-1})(\sigma(\mathbf{x}_0))_{ij} (D\sigma(\mathbf{x}_0)\xi)_i (D\sigma(\mathbf{x}_0)\eta)_j, \quad (3)$$

where $\sigma : U \rightarrow \mathbb{R}^n$ is any chart around $\mathbf{x}_0 \in M$ and $\tilde{H}(f \circ \sigma^{-1})$ denotes the ordinary Hesse matrix of the chart representation $f \circ \sigma^{-1}$. It is straightforward to show that (3)

⁵see Subsec. 2.3 below

is independent of σ . Moreover, we will call \mathbf{x}_0 a *strict saddle point* if $H_f(\mathbf{x}_0)$ (or more precisely the associated symmetric operator) has at least one negative eigenvalue.

The above concepts allow a trivial generalization of a well-known result from elementary calculus which follows straightforwardly in local coordinates.

Proposition 2.3. *Let M be a Riemannian manifold and let \mathbf{x} be a critical point of the smooth function $f : M \rightarrow \mathbb{R}$. If $H_f(\mathbf{x})$ is positive definite, then \mathbf{x} is a strict local minimum of f .*

Now the question arises whether the (asymptotic) stability of an equilibrium $\mathbf{x} \in M$ of (2) may depend on the Riemannian metric \mathbf{g} — and the answer is surprisingly “yes”, cf. Takens (1971). However, certain properties such as being a strict local minimum or an isolated critical point are obviously not up to the choice of the metric, and thus the (asymptotic) stability of those equilibria is independent of the Riemannian metric as the next theorem shows.

Theorem 2.4. *Let M be a Riemannian manifold and $f : M \rightarrow \mathbb{R}$ a smooth function. Then the following hold:*

- (i) *Every strict local minimum of f is a stable equilibrium of (2).*
- (ii) *Every strict local minimum of f which is additionally an isolated critical point is an asymptotically stable equilibrium of (2).*

Both assertions follow immediately from classical stability theory by taking f as Lyapunov function, cf. Helmke and Moore (1994); Irwin (1980). Handling non-isolated critical points is much more subtle. A first hint on how to approach this issue is obtained by Cor. 2.2 which could be restated (in a slightly weaker version) as follows:

For Morse functions with compact sublevel sets every solution of the corresponding gradient system converges (for $t \rightarrow \infty$) to a single critical point.

This suggests to work with Morse–Bott functions when it comes to non-isolated critical points. Recall that a smooth function $f : M \rightarrow \mathbb{R}$ is called a *Morse–Bott function*, if the set C of critical points is a closed submanifold of M , such that its tangent space $T_{\mathbf{x}}C$ coincides with the kernel of the Hessian operator for all $\mathbf{x} \in C$. Note that C is allowed to have several connected components with possibly different dimensions, (Helmke and Moore, 1994, p. 366), (Nicolaescu, 2011, Def. 2.41) or Banyaga and Hurtubise (2010). Thus Morse functions are particular Morse–Bott functions, where C consists only of 0-dimensional manifolds (i.e. isolated points).

Now, the above concept allows a generalization of the Morse–Palais Lemma to Morse–Bott functions which is often called Morse–Bott Lemma, see Banyaga and Hurtubise (2004). It yields a local normal form of Morse–Bott functions near their critical points, which reads in local coordinates as follows

$$\tilde{f}(\mathbf{x}, \mathbf{y}, \mathbf{z}) = \|\mathbf{x}\|^2 - \|\mathbf{y}\|^2,$$

with $\mathbf{x} \in \mathbb{R}^{n_+}$, $\mathbf{y} \in \mathbb{R}^{n_-}$, and $\mathbf{z} \in \mathbb{R}^{n_0}$, where n_+ , n_- and n_0 are the numbers of positive, negative and zero eigenvalues of the Hessian operator respectively. Here $\|\cdot\|^2$ denotes the usual Euclidean norm. This finally allows to prove that solutions of the respective gradient system converge to a single critical point.

Theorem 2.5 (Thm. 2.3 in [Aulbach \(1984\)](#)). *Let $f : M \rightarrow \mathbb{R}$ be a Morse–Bott function on a Riemannian manifold M with compact sublevel sets. Then every solution of the gradient flow (2) converges to a single critical point. Moreover, for almost every initial point, the flow converges to a local minimum.*

Finally, we recall another very powerful result for analyzing the convergence of gradient systems which is based on Łojasiewicz’s celebrated gradient estimate [Łojasiewicz \(1984\)](#). Let $f : M \rightarrow \mathbb{R}$ be real analytic, $\mathbf{x}_0 \in M$ a critical point of f , and assume without loss of generality that $f(\mathbf{x}_0) = 0$. Then, near \mathbf{x}_0 , one has the estimate

$$\|\text{grad}(\mu \circ f)(\mathbf{x})\| \geq c, \quad (4)$$

where $\mu : \mathbb{R}^+ \rightarrow \mathbb{R}^+$ is a strictly increasing C^1 -function and $c > 0$ some positive constant, cf. ([Lageman, 2007](#), Cor. 1.1.25). In the literature, one usually finds $\mu(r) := r^{1-\theta}$ with $\theta \in (0, 1)$. Eq. (4) easily allows to bound the length of any trajectory of (2) whose ω -limit set is non-empty. Hence one gets the following result.

Theorem 2.6 ([Łojasiewicz \(1984\)](#)). *Let (M, g) and $f : M \rightarrow \mathbb{R}$ be real analytic. Then every non-empty ω -limit set of (2) consists only of a single critical point.*

2.4 The Exponential Map and Numerical Gradient Descent

Finally, we approach the problem of discretization of (2) resulting in a convergent gradient descent method (cp. Fig.1). The ideas presented here can be traced back to [Brockett \(1988, 1989\)](#) and [Smith \(1993, 1994\)](#). Let

$$\exp_{\mathbf{x}} : T_{\mathbf{x}}M \rightarrow M \quad (5)$$

denote the *Riemannian exponential map* at $\mathbf{x} \in M$, i.e. $t \rightarrow \exp_{\mathbf{x}}(t\xi)$ is the unique geodesic with initial value $\mathbf{x} \in M$ and initial velocity $\xi \in T_{\mathbf{x}}M$. Here, we assume for simplicity that (M, g) is (geodesically) complete, i.e. (5) is well-defined for the entire tangent space $T_{\mathbf{x}}M$. Probably the simplest discretization scheme given by

$$\mathbf{x}_{k+1} := \exp_{\mathbf{x}_k}(-\eta_k \text{grad } f(\mathbf{x}_k)), \quad (6)$$

can be seen as a “natural” generalization of the explicit Euler method. Here $\eta_k > 0$ denotes an appropriate “step size”⁶ which may depend on $k \in \mathbb{N}$.

Remark 2.7. *It should be mentioned that gradient descent algorithms are usually studied as exact algorithms, not as numerical algorithms where real numbers are represented as floating point values and arithmetic is not exact. Numerical effects can be important, for instance cancellation effects from computing gradients in a naive way [Muller et al \(2018\)](#). Nevertheless, this paper will ignore these numerical issues.*

In order to guarantee convergence of (6) to the set of critical points, it is sufficient to apply the Armijo rule, see [Luenberger and Ye \(2008\)](#). An alternative to Armijo’s

⁶Note that the “actual” step size results from the modulus of $\eta \text{grad } f(\mathbf{x}_k)$.

rule provides the step-size selection suggested by [Brockett \(1993\)](#), see also [Helmke and Moore \(1994\)](#). Moreover, for compact Riemannian manifolds even a sufficiently small constant step size $\eta > 0$ guarantees convergence:

Theorem 2.8. *If f has compact sublevel sets, every trajectory of the discretized gradient descent (6) (with constant but small enough step size) converges to the set of critical points. Moreover, if additionally*

- (i) *all critical points are isolated, then any trajectory of (6) converges to a single critical point of f .*
- (ii) *all saddle points are strict, then the set of initial points converging to strict saddle points has measure zero (in the sense of Sec. 2.1).*

Part (ii) of the above statement can be found in ([Lee et al, 2019](#), Cor. 6).⁷ Thus, for a function with compact sublevel sets, gradient descent (6) behaves similarly to its continuous counter-part, cf. Prop. 2.1 and Cor. 2.2, i.e. it converges almost surely to a local minimum if the step size is chosen small enough.

Deeper results, which yield convergence to a single critical point, are more subtle to derive. Here we present one result in this direction which is again based on the analyticity of the cost function f and on Łojasiewicz’s inequality.

Theorem 2.9. [Lageman \(2007\)](#) *If (M, g) and f are real analytic, and the step sizes are chosen according to a version of the first Wolfe–Powell condition for Riemannian manifolds, then pointwise convergence holds.*

Finally, in order to determine the largest admissible step size of our algorithm, we need a notion of Lipschitz continuity of vector fields on Riemannian manifolds. Care has to be taken here since tangent vectors in different tangent spaces cannot be compared by default. Certainly, one can define local Lipschitz continuity via local charts but this does not allow to assign a meaningful Lipschitz constant to the vector field. A natural and intrinsic way to do this is to define Lipschitz continuity via parallel transport along the unique connecting geodesic, as is done in [Fetecau and Patacchini \(2022\)](#).

Definition 2.10. *Let (M, g) be a complete Riemannian manifold and let X be a vector field on M . We say that X is ℓ -Lipschitz if for all $\mathbf{x}, \mathbf{y} \in M$ with⁸ $d(x, y) \leq r_M$ it holds that⁹ $\|X(\mathbf{x}) - \Pi_{\mathbf{y}, \mathbf{x}} X(\mathbf{y})\|_{\mathbf{x}} \leq \ell d(\mathbf{x}, \mathbf{y})$. If $f : M \rightarrow \mathbb{R}$ is a differentiable function, then we say that f is ℓ -smooth if $\text{grad}(f)$ is ℓ -Lipschitz.*

Note that this definition is slightly broader than the definition given in [Fetecau and Patacchini \(2022\)](#).

⁷There the authors consider Riemannian manifolds embedded in the Euclidean space and retractions instead of an intrinsic Riemannian exponential function, but this does not restrict the generality of the result, cf. the Nash embedding theorem ([Berger, 2003](#), Thm. 46).

⁸Here r_M stands for the injectivity radius of M .

⁹Here $\Pi_{\mathbf{y}, \mathbf{x}}$ denotes the parallel transport from \mathbf{y} to \mathbf{x} along the unique length minimizing geodesic connecting the two points.

3 Algorithm and Convergence

We will study the following randomly projected gradient descent algorithm (cp. Fig. 1). Given a Riemannian manifold M of dimension N , an initial state $\mathbf{x}_0 \in M$, a smooth function $f : M \rightarrow \mathbb{R}$, and a step size $\eta > 0$ (with upper bound to be determined), the update rule is given by

$$\mathbf{x}_{i+1} = \exp_{\mathbf{x}_i}(-\eta g(\mathbf{x}_i, \mathbf{u}_i)), \quad g(\mathbf{x}, \mathbf{u}) = \langle \mathbf{u}, \text{grad } f(\mathbf{x}) \rangle \mathbf{u}, \quad \mathbf{S}_{\mathbf{x}_i} M \ni \mathbf{u}_i \stackrel{\text{i.i.d.}}{\sim} \mathcal{P}(\mathbf{x}_i), \quad (7)$$

where $\mathbf{S}_{\mathbf{x}} M$ denotes the unit sphere in the tangent space $\mathbf{T}_{\mathbf{x}} M$ and $\mathcal{P}(\mathbf{x}_i)$ some probability distribution on the unit sphere $\mathbf{S}_{\mathbf{x}_i} M$. (Recall that “i.i.d.” stands for “independent and identically distributed”). Intuitively, the gradient is projected onto a randomly chosen direction \mathbf{u} at each step. Throughout this paper we will consider two cases:

- (I) Either $\mathcal{P}(\mathbf{x}_i) = \mathcal{U}(\mathbf{S}_{\mathbf{x}_i} M)$ denotes the uniform (rotationally invariant) probability distribution on the unit sphere, also called Haar measure;
- (II) or $\mathcal{P}(\mathbf{x}_i) = \mathcal{D}(\mathbf{S}_{\mathbf{x}_i} M)$ denotes a finite probability distribution on the unit sphere accessing all possible directions in the sense of Assumption 3.1.

Assumption 3.1 (Discrete case). *Given k continuous vector fields ξ_1, \dots, ξ_k and k continuous weights p_1, \dots, p_k on M with $p_j \geq 0$ and $\sum_{j=1}^k p_j \equiv 1$, such that $p_j \xi_j / \|\xi_j\|$ is continuous, where the expression is set to zero when it is undefined. This implies for instance that $p_j(\mathbf{x}) = 0$ whenever $\xi_j(\mathbf{x}) = 0$.*

Then \mathbf{u}_i takes value $\xi_j(\mathbf{x}_i) / \|\xi_j(\mathbf{x}_i)\|$ with probability $p_j(\mathbf{x}_i)$. Moreover, we suppose that at every point \mathbf{x} , the tangent vectors $p_1(\mathbf{x})\xi_1(\mathbf{x}), \dots, p_k(\mathbf{x})\xi_k(\mathbf{x})$ span the entire tangent space even after removing any single vector $p_j(\mathbf{x})\xi_j(\mathbf{x})$ and, if present, all its scalar multiples.

The following technical lemma will be useful later.

Lemma 3.2. *Let K be a compact subset of a manifold M , and let $\{v_j\}_{j=1}^k$ be a set of continuous vector fields on K which span the tangent space at every point. Then, for any continuous, non-vanishing vector field v on K there is some $\varepsilon > 0$ such that*

$$\min_{\mathbf{x} \in K} \max_{j=1, \dots, k} |\langle v_j(\mathbf{x}), v(\mathbf{x}) \rangle| = \varepsilon.$$

Proof. The functions $\mathbf{x} \mapsto |\langle v_j(\mathbf{x}), v(\mathbf{x}) \rangle|$ defined on K are continuous and non-negative. Hence their maximum over j is still a continuous non-negative function on K . Since the v_j span each tangent space, this function is even strictly positive, and by compactness of K , there is a positive global minimum. \square

Note that a related condition is used in (Gutman and Ho-Nguyen, 2023, Thm. 5.2) to guarantee convergence to the set of critical points.

Our goal is to analyze the convergence behavior of this algorithm, and in particular, to show that it converges almost surely to a local minimum of f . A deterministic version of the above described algorithm (in the sense that all “perturbations” from the

classical gradient descent are deterministic and not random) was analyzed in (Absil et al, 2008, Def. 4.2.1, Thm. 4.3.1) under the heading “gradient-related methods”.

3.1 Basic Properties

We start with some simple properties of the function g defined in (7).

Lemma 3.3. *Let $\mathbf{x} \in M$ be given. If $\mathbf{u} \in \mathbf{S}_{\mathbf{x}}M$, then it holds that*

$$\langle \text{grad } f(\mathbf{x}), g(\mathbf{x}, \mathbf{u}) \rangle = \|g(\mathbf{x}, \mathbf{u})\|^2.$$

Proof. Using the definition of $g(\mathbf{x}, \mathbf{u})$ and the fact that \mathbf{u} is a unit vector, we immediately obtain $\langle \text{grad } f(\mathbf{x}), g(\mathbf{x}, \mathbf{u}) \rangle = \langle \mathbf{u}, \text{grad } f(\mathbf{x}) \rangle^2 = \|g(\mathbf{x}, \mathbf{u})\|^2$. \square

Corollary 3.4. *Note that if \mathbf{u} is uniformly distributed (w.r.t. the Haar measure) on the sphere, then*

$$\langle \mathbf{u}, \text{grad } f(\mathbf{x}) \rangle^2 \stackrel{d}{=} u_N^2 \|\text{grad } f(\mathbf{x})\|^2,$$

where $\stackrel{d}{=}$ means that the random variables have the same distribution, and u_N denotes the N -th coordinate of \mathbf{u} .

Remark 3.5. *The image of the function $\mathbf{u} \mapsto g(\mathbf{x}, \mathbf{u})$ is a hypersphere in $\mathbf{T}_{\mathbf{x}}M$ with center $\frac{1}{2} \text{grad } f(\mathbf{x})$ and intersecting the origin: Indeed, let $\mathbf{x} \in M$ be fixed and consider the map $g_{\mathbf{x}} : \mathbf{S}_{\mathbf{x}}M \rightarrow \mathbf{T}_{\mathbf{x}}M$ given by $\mathbf{u} \mapsto g(\mathbf{x}, \mathbf{u})$. To simplify formulas, we choose an orthonormal basis (e_1, \dots, e_N) in $\mathbf{T}_{\mathbf{x}}M$ such that $\text{grad } f(\mathbf{x}) = \|\text{grad } f(\mathbf{x})\| e_N$. In such coordinates the map $g_{\mathbf{x}}$ is given by*

$$g_{\mathbf{x}}(u_1, \dots, u_N) = u_N \|\text{grad } f(\mathbf{x})\| (u_1, \dots, u_N).$$

A straightforward computation shows that $\|(u_N u_1, \dots, u_N^2 - \frac{1}{2})\| = \frac{1}{2}$, and so the image of $g_{\mathbf{x}}$ lies on a sphere with center $\frac{1}{2} \text{grad } f(\mathbf{x})$ and passing through the origin. This induces a probability measure on the image. Consider the function

$$\tilde{g}(\mathbf{x}, \mathbf{v}) = \frac{1}{2}(\text{grad } f(\mathbf{x}) + \mathbf{v} \|\text{grad } f(\mathbf{x})\|),$$

and let \mathbf{v} be distributed on the unit sphere according to a probability measure $\mathcal{V}(\mathbf{S}_x M)$ such that g and \tilde{g} induce the same probability measure. The measure \mathcal{V} is not uniform on the sphere, but it is still invariant under rotations preserving $\text{grad } f(\mathbf{x})$. We see that $v_N \sim 2u_N^2 - 1$. More details on the distribution of u_N and u_N^2 can be found in Lems. A.1 and A.2.

Note that since the standard deviation of u_N^2 is larger than the expected value, Chebyshev’s inequality cannot be applied to obtain useful concentration bounds. For large dimension N , there exist good approximations of these distributions. In fact, the distribution of a coordinate of a uniformly random unit vector approximately follows a normal distribution, and hence its square approximates a χ_1^2 distribution. See Lem. A.2 for a precise result.

Corollary 3.6. *If $\mathbb{E}[\mathbf{u}\mathbf{u}^\top] = \mathbf{I}_N/N$, which is satisfied for the Haar measure, then it holds that*

$$\mathbb{E}[g(\mathbf{x}, \mathbf{u})] = \frac{\text{grad } f(\mathbf{x})}{N}$$

for any $\mathbf{x} \in M$.

Proof. We compute: $\mathbb{E}[g(\mathbf{x}, \mathbf{u})] = \mathbb{E}[\mathbf{u}\mathbf{u}^\top \text{grad } f(\mathbf{x})] = \frac{1}{N} \text{grad } f(\mathbf{x})$. \square

The corollary shows that in this case the projected gradient is of size $\text{grad } f(\mathbf{x})/N$, and hence it is rather small for large N . Intuitively, this happens because in high dimensions, a uniformly random unit vector u will be close to orthogonal to the gradient with high probability — after all, there are $N - 1$ dimensions which are orthogonal to the gradient.

Now that we better understand the iteration rule, we want to understand by what amount the objective function value is likely to decrease after a certain number of iterations. It will be useful to use normal coordinate charts at the current point \mathbf{x}_i . These charts satisfy that the metric at the origin is trivial, and that geodesics passing through the origin are straight and uniformly parametrized, see for instance (Lee, 2013, Prop. 5.24). In particular, when using a normal coordinate chart about \mathbf{x}_i , the random variable \mathbf{x}_{i+1} , conditioned on \mathbf{x}_i , is still distributed on a hypersphere.

Lemma 3.7. *Let (M, g) be compact with injectivity radius r_M and let $f : M \rightarrow \mathbb{R}$ be ℓ -smooth. Then for $\eta \leq \min(1/\ell, r_M)$ it holds that*

$$f(\mathbf{x}_{i+1}) - f(\mathbf{x}_i) \leq -\eta \left(1 - \frac{\ell\eta}{2}\right) \langle \text{grad } f(\mathbf{x}_i), g(\mathbf{x}_i, \mathbf{u}_i) \rangle \leq 0.$$

In particular the function value is surely non-increasing.

Proof. We choose a normal coordinate chart about \mathbf{x}_i and denote the coordinates by $\tilde{\mathbf{x}}$ and the function in coordinates by \tilde{f} . In particular $\tilde{\mathbf{x}}_i = 0$. Note that at the origin $\text{grad } \tilde{f}(\tilde{\mathbf{x}}_i) = \nabla \tilde{f}(\tilde{\mathbf{x}}_i)$ and the coordinate representation of $\mathbf{x}_{i+1} = \exp_{\mathbf{x}_i}(-\eta g(\mathbf{x}_i, \mathbf{u}_i))$ is given by $\tilde{\mathbf{x}}_{i+1} = -\eta \tilde{g}(\mathbf{x}_i, \mathbf{u}_i)$, where $\tilde{g}(\mathbf{x}_i, \mathbf{u}_i)$ is the chart representation of $g(\mathbf{x}_i, \mathbf{u}_i)$. Then, by the proof of (Nesterov, 2004, Lemma 1.2.3) and Lem. 3.3, it holds that

$$\begin{aligned} f(\mathbf{x}_{i+1}) - f(\mathbf{x}_i) &= \tilde{f}(\tilde{\mathbf{x}}_{i+1}) - \tilde{f}(\tilde{\mathbf{x}}_i) \\ &\leq \langle \nabla \tilde{f}(\tilde{\mathbf{x}}_i), \tilde{\mathbf{x}}_{i+1} - \tilde{\mathbf{x}}_i \rangle + \frac{\ell}{2} \|\tilde{\mathbf{x}}_{i+1} - \tilde{\mathbf{x}}_i\|^2 \\ &\leq -\eta \langle \text{grad } f(\mathbf{x}_i), g(\mathbf{x}_i, \mathbf{u}_i) \rangle + \frac{\ell\eta^2}{2} \|g(\mathbf{x}_i, \mathbf{u}_i)\|^2 \\ &= -\eta \left(1 - \frac{\ell\eta}{2}\right) \langle \text{grad } f(\mathbf{x}_i), g(\mathbf{x}_i, \mathbf{u}_i) \rangle, \end{aligned}$$

as desired. \square

This result shows that, under the assumptions of Cor. 3.6, we obtain the conditional expectation

$$\mathbb{E}[f(\mathbf{x}_{i+1}) - f(\mathbf{x}_i) \mid \mathbf{x}_i] \leq -\frac{\eta}{N} \left(1 - \frac{\ell\eta}{2}\right) \|\text{grad } f(\mathbf{x}_i)\|^2.$$

More generally the previous result shows that the only way for the algorithm to stop improving is for the gradient to vanish: $\text{grad } f(\mathbf{x}_i) \rightarrow 0$ as $i \rightarrow \infty$.

Corollary 3.8. *Under the assumptions of Lem. 3.7, the function values converge (surely) to some value c . Moreover, the following assertions hold almost surely*

- (i) c is a critical value of f .
- (ii) \mathbf{x}_i converges to the critical set of c , i.e. to the set of critical point with $f(\mathbf{x}) = c$.

Proof. By Lem. 3.7 the function values are non-increasing and bounded below, hence they converge to some value c . We will show that $\Pr(\text{grad } f(\mathbf{x}_i) \not\rightarrow 0) = 0$, which immediately implies the result. Since $f(\mathbf{x}_{i+1}) - f(\mathbf{x}_i) \rightarrow 0$, Lem. 3.7 shows that $\langle \text{grad } f(\mathbf{x}_i), g(\mathbf{x}_i, \mathbf{u}_i) \rangle \rightarrow 0$.

Note that if $\text{grad } f(\mathbf{x}_i) \not\rightarrow 0$, then there is some $m \in \mathbb{N}$ such that $\|\text{grad } f(\mathbf{x}_i)\| > \frac{1}{m}$ on some infinite subsequence. Let $z_j^m = \langle \mathbf{u}_{i(j)}, \text{grad } f(\mathbf{x}_{i(j)}) \rangle / \|\text{grad } f(\mathbf{x}_{i(j)})\|$ where $i(j)$ is the j -th index such that $\|\text{grad } f(\mathbf{x}_{i(j)})\| \geq \frac{1}{m}$. Note that

$$\langle \text{grad } f(\mathbf{x}_{i(j)}), g(\mathbf{x}_{i(j)}, \mathbf{u}_{i(j)}) \rangle = (z_j^m \|\text{grad } f(\mathbf{x}_{i(j)})\|)^2.$$

Hence, if the gradients do not converge to 0, then, for some m , it must hold that $|z_j^m| \rightarrow 0$.

We claim that there exist $0 < \varepsilon, \delta < 1$ such that for all $\mathbf{x} \in M$ with $f(\mathbf{x}) \leq f(\mathbf{x}_0)$ it holds that

$$\Pr(|\langle \mathbf{u}, \text{grad } f(\mathbf{x}) \rangle| \leq \varepsilon \|\text{grad } f(\mathbf{x})\|) \leq \delta.$$

If $\mathbf{u} \sim \mathcal{U}(\mathbf{S}_{\mathbf{x}}M)$ this follows from Lem. A.1, if $\mathbf{u} \sim \mathcal{D}(\mathbf{S}_{\mathbf{x}}M)$ this follows from Lem. 3.2.

Given $m, n, k \in \mathbb{N}$ with $1/n < \varepsilon$, and using the chain rule, Markovianity, and the claim above, we compute that

$$\Pr(\forall j > k : |z_j^m| \leq \frac{1}{n}) = \prod_{j=k}^{\infty} \Pr(|z_j^m| \leq \frac{1}{n} \mid \forall l \in \{j, \dots, k\} : |z_l^m| \leq \frac{1}{n}) = 0.$$

For any fixed value of n , we can use a union bound over all $m, k \geq 1$ and obtain

$$\Pr(\exists m, k \forall j > k : |z_j^m| \leq \frac{1}{n}) = 0,$$

which implies that

$$\Pr(\exists m : |z_j^m| \rightarrow 0 \text{ as } j \rightarrow \infty) = 0,$$

as desired. □

3.2 Escaping Saddle Points

The main difficulty in proving almost sure convergence to a local minimum of the randomly projected gradient descent algorithm is to show that it does not get stuck in a saddle point.

Recall from Lem. 3.7 that the function value cannot increase. Hence, once we cross the critical value corresponding to some saddle point, we say that we have *passed* the saddle point, as now it is impossible to converge to the saddle point in question.

We start by proving the result in a simplified “isotropic” case, before treating the general case as a perturbation.

Lemma 3.9. *Consider the function $f : \mathbb{R}^N \rightarrow \mathbb{R}$ defined by*

$$f(x, y, z) = a_1 x_1^2 + \dots + a_p x_p^2 - (b_1 y_1^2 + \dots + b_q y_q^2),$$

with $x \in \mathbb{R}^p$, $y \in \mathbb{R}^q$, $z \in \mathbb{R}^{N-p-q}$, and $p, q \geq 1$ as well as $a_i, b_j > 0$. Then f is ℓ -smooth with $\ell = 2 \max\{a_1, \dots, a_p, b_1, \dots, b_q\}$. Moreover, let $0 < \eta \leq \frac{1}{\ell}$ and define

$$\theta := \arctan\left(\frac{b_1 y_1^2 + \dots + b_q y_q^2}{a_1 x_1^2 + \dots + a_p x_p^2}\right) \in [0, \frac{\pi}{2}] \quad \text{for } (x_1, \dots, x_p, y_1, \dots, y_q) \neq 0. \quad (8)$$

Then there exist constants $\varepsilon, \delta > 0$ such that for all¹⁰ $\theta \in [0, \frac{\pi}{3}]$ it holds that

$$\Pr(\theta_{i+1} - \theta_i \geq \varepsilon) \geq \delta.$$

Proof. The negative gradient of f is

$$\begin{aligned} -\nabla f(x_1, \dots, x_p, y_1, \dots, y_q, z_1, \dots, z_{N-p-q}) \\ = -2(a_1 x_1, \dots, a_p x_p, -b_1 y_1, \dots, -b_q y_q, 0, \dots, 0) \end{aligned}$$

and the value of ℓ follows immediately. A key property of this simplified setting is that the gradient is a linear vector field on \mathbb{R}^N , and so the entire situation is invariant under scaling. Moreover, from the definition of θ it is clear that f vanishes if and only if $\theta = \frac{\pi}{4}$ or $(x_1, \dots, x_p, y_1, \dots, y_q) = 0$. Due to the scaling invariance of the algorithm and of (8), we may focus on an initial point $\mathbf{x}_i = (x_i, y_i, z_i)$ on the unit sphere S^{N-1} . After executing one step, we obtain a random improvement of our angle, namely $\theta_{i+1} - \theta_i$ which depends on \mathbf{u}_i appearing in the update rule.

First let us consider this improvement in the uniform Case (I) as a function of \mathbf{x}_i and \mathbf{u}_i , i.e.,

$$h(\mathbf{x}_i, \mathbf{u}_i) := \theta_{i+1} - \theta_i.$$

It is clear that this is a continuous function. The optimal improvement achievable for a given \mathbf{x}_i is found by maximizing over \mathbf{u}_i . One can show that the resulting function is still continuous in \mathbf{x}_i . Moreover we claim that it is strictly positive on the compact set $K_{\pi/3} := \{\mathbf{x} \in S^{n-1} : \theta(\mathbf{x}) \leq \pi/3\}$. Indeed, if $\theta_i > 0$, then this follows from the

¹⁰The value $\frac{\pi}{3}$ is arbitrary and could be replaced by any other value in $(\frac{\pi}{4}, \frac{\pi}{2})$ without changing the proof.

choice of η . If we perform a single (deterministic) negative gradient step with step size η , none of the coordinates will change sign, and whenever $\theta_i \in (0, \frac{\pi}{3}]$ its value will strictly increase. If $\theta_i = 0$, it is clear that the value of θ_i will almost surely strictly increase, as the set of points \mathbf{x}_{i+1} with $\theta_{i+1} = 0$ form a strict subspace of \mathbb{R}^n . Taken together this shows that there is some $\varepsilon > 0$ such that the optimal improvement is at least 2ε for every initial $\mathbf{x}_i \in K_{\pi/3}$.

It follows that for any given initial state $\mathbf{x}_i \in K_{\pi/3}$, the probability that $\theta_{i+1} - \theta_i \geq \varepsilon$ is strictly positive. Indeed, $h(\mathbf{x}_i, \cdot)$ is a continuous function on this sphere and its preimage of $(\varepsilon, +\infty)$ on the sphere is a non-empty open set and hence has a strictly positive probability (with respect to the Haar measure). Moreover one can show that this probability depends continuously on the initial state \mathbf{x}_i , and again we obtain a positive minimum δ on the K_θ by compactness. This proves that $\Pr(\theta_{i+1} - \theta_i \geq \varepsilon) \geq \delta$ independently of the initial state $\mathbf{x} \in K_{\pi/3}$.

Next consider the discrete Case (II). Again we need to prove that there exist constants $\varepsilon, \delta > 0$ such that for all $\theta \in [0, \frac{\pi}{3}]$ it holds that $\Pr(\theta_{i+1} - \theta_i \geq \varepsilon) \geq \delta$. The only cases where $h(\mathbf{x}, \mathbf{u}) = 0$ (note that it cannot be negative) with probability one is when all $v_j(\mathbf{x})$ for $j = 1, \dots, k$ are either orthogonal to $\text{grad}(\mathbf{x})$ or collinear to \mathbf{x} . By Assumption 3.1, this cannot happen. Hence $\max_j h(\mathbf{x}, \mathbf{v}_j)$ is non-negative and continuous, and on the compact set $K_{\pi/3}$ it is even strictly positive. This concludes the proof. \square

As a corollary, we are able to show that after sufficiently many steps, the algorithm passes the saddle point with high probability.

Corollary 3.10. *In the same setting as above, there exist $\varepsilon, \delta > 0$ such that, with $n = \lceil \frac{\pi}{3\varepsilon} \rceil$, we have that*

$$\Pr(\theta_n \geq \frac{\pi}{3}) \geq \delta^n.$$

It follows that for any $m \in \mathbb{N}$, it holds that

$$\Pr(\theta_{mn} < \frac{\pi}{3}) \leq \Pr(\theta_n < \frac{\pi}{3})^m \leq (1 - \delta^n)^m,$$

which goes to 0 as $m \rightarrow \infty$.

Proof. It follows immediately from Lem. 3.9 that in n steps we achieve $\Pr(\theta_{i+n} - \theta_i \geq n\varepsilon) \geq \delta^n$, or put differently, setting $n = \lceil \frac{\pi}{3\varepsilon} \rceil$, we get

$$\Pr(\theta_n \geq \frac{\pi}{3}) \geq \Pr(\theta_n \geq n\varepsilon) \geq \delta^n = \delta^{\lceil \frac{\pi}{3\varepsilon} \rceil} > 0.$$

This proves the first statement. The second statement follows from the Markovianity of the process. \square

In order to generalize Cor. 3.10 to the desired setting we will treat the effects of the Riemannian metric and the higher order terms of f as a perturbation on the algorithm. We start with the following general perturbation result.

Lemma 3.11. *Let G be a linear vector field on \mathbb{R}^n and let $\eta > 0$ be given. Moreover let P be any other vector field on \mathbb{R}^n satisfying $\|P(\mathbf{x})\| \leq C\|\mathbf{x}\|^2$ for some $C > 0$. Then it holds that*

$$\|\mathbf{x} - \eta G\mathbf{x} - (\mathbf{y} - \eta(G + P)\mathbf{y})\| \leq \|\mathbb{1} + \eta G\| \|\mathbf{x} - \mathbf{y}\| + C\eta\|\mathbf{y}\|^2,$$

where $\|\mathbb{1} + \eta G\|$ denotes the operator norm. Let $\mathbf{x}_{i+1} = \mathbf{x}_i - \eta G\mathbf{x}_i$ and $\mathbf{y}_{i+1} = \mathbf{y}_i - \eta(G + P)\mathbf{y}_i$. Hence after n steps, if the states remain in an R -ball about the origin, then

$$\|\mathbf{x}_{i+n} - \mathbf{y}_{i+n}\| \leq \|\mathbb{1} + \eta G\|^n \left(\|\mathbf{x}_i - \mathbf{y}_i\| + \frac{CR^2}{\|\mathbb{1} + \eta G\| - 1} \right).$$

Proof. The first inequality follows from the assumptions using the triangle inequality:

$$\begin{aligned} \|\mathbf{x} - \eta G\mathbf{x} - (\mathbf{y} - \eta(G + P)\mathbf{y})\| &= \|(\mathbb{1} + \eta G)(\mathbf{x} - \mathbf{y}) + \eta P(\mathbf{y})\| \\ &\leq \|\mathbb{1} + \eta G\| \|\mathbf{x} - \mathbf{y}\| + C\eta\|\mathbf{y}\|^2. \end{aligned}$$

Now using the assumption that $\|\mathbf{y}\| \leq R$, and by iterating this result for n steps, we find that

$$\begin{aligned} \|\mathbf{x}_{i+n} - \mathbf{y}_{i+n}\| &\leq \|\mathbb{1} + \eta G\|^n \|\mathbf{x}_i - \mathbf{y}_i\| + (\|\mathbb{1} + \eta G\|^{n-1} + \dots + 1)CR^2 \\ &\leq \|\mathbb{1} + \eta G\|^n \left(\|\mathbf{x}_i - \mathbf{y}_i\| + \frac{CR^2}{\|\mathbb{1} + \eta G\| - 1} \right). \end{aligned}$$

This concludes the proof. \square

In our case, we can always choose coordinates in which the problem locally looks like the setting of Lem. 3.9 with a perturbation as in Lem. 3.11.

Lemma 3.12. *Let (M, g) be a Riemannian manifold and let $f : M \rightarrow \mathbb{R}$ be a Morse–Bott function on M . If $\mathbf{x}_0 \in M$ is a critical point of f , then there exists a chart $\sigma : U \rightarrow \mathbb{R}^n$ about \mathbf{x}_0 such that, with $\tilde{\mathbf{x}} = \sigma(\mathbf{x}) = (x_1, \dots, x_p, y_1, \dots, y_q, z_1, \dots, z_{N-p-q})$,*

$$\begin{aligned} \sigma(\mathbf{x}_0) &= 0, \\ f \circ \sigma^{-1}(\tilde{\mathbf{x}}) &= c + a_1 x_1^2 + \dots + a_p x_p^2 - (b_1 y_1^2 + \dots + b_q y_q^2) + \mathcal{O}(\|\tilde{\mathbf{x}}\|^2), \\ g_{ij}(\tilde{\mathbf{x}}) &= \delta_{ij} + \mathcal{O}(\|\tilde{\mathbf{x}}\|), \end{aligned}$$

where δ_{ij} denotes the Kronecker symbol.

Proof. Choose coordinates about \mathbf{x}_0 such that the metric is Euclidean at $\tilde{\mathbf{x}}_0$ (e.g. normal coordinates), then use an orthogonal transformation to diagonalize the Hessian of f at $\tilde{\mathbf{x}}_0$. \square

Now we can combine the three previous results.

Corollary 3.13. *Let M be a Riemannian manifold and let f be a Morse–Bott function on M . For any strict saddle point $\mathbf{x} \in M$ with value $f(\mathbf{x}) = c$ there exists $N > 0$ and a neighborhood U of \mathbf{x} such that*

$$\Pr(f(\mathbf{x}_{i+N}) < c \mid \mathbf{x}_i, \dots, \mathbf{x}_{i+N} \in U) > \delta.$$

Proof. This follows immediately from Cor. 3.10, Lem. 3.11 and Lem. 3.12. \square

Lemma 3.14. *Let M be a Riemannian manifold and let f be a Morse–Bott function on M . Further assume that $f : M \rightarrow \mathbb{R}$ has compact sublevel sets and that $\mathbf{x}_0 \in M$ is not a critical point of f . Then the probability that \mathbf{x}_i converges to the set of strict saddle points as $i \rightarrow \infty$ is zero.*

Proof. Let C be the set of all strict saddle points \mathbf{x} with $f(\mathbf{x}) \leq f(\mathbf{x}_0)$. By assumption on f the set C is compact; actually, C consists of finitely many connected compact submanifolds, cf. (Nicolaescu, 2011, Def. 2.41). We will show that the probability that \mathbf{x}_i converges to C is zero. Note that by Lem. 3.7 the function value is (surely) not increasing, and therefore we can focus on $C_c := C \cap f^{-1}(c)$ for some $c \leq f(\mathbf{x}_0)$. By compactness of C_c we can choose for each $\mathbf{z} \in C_c$ balls $B_{r_z}(\mathbf{z})$, $B_{R_z}(\mathbf{z})$ around \mathbf{z} with $r_z < R_z$ such that both balls are contained in a neighborhood $U(\mathbf{z})$ of \mathbf{z} as in Cor. 3.13 and such that any realization \mathbf{x}_i needs at least N steps to transverse the spherical shells $B_{R_z}(\mathbf{z}) \setminus B_{r_z}(\mathbf{z})$. Since C_c is compact we can find a finite covering by balls of the form $B_{r_z/2}(\mathbf{z})$, i.e.

$$C_c \subset \bigcup_{k=1}^K B_{r_k/2}(\mathbf{z}_k),$$

Next define $r_* := \min_{k=1, \dots, K} r_k/2$. Then, by assumption, there exists some $L \in \mathbb{N}$ such that $d(\mathbf{x}_i, C_c) < r_*$ for all $i \geq L$. Hence we conclude $d(\mathbf{x}_L, \mathbf{z}) \leq r_*$ for some $\mathbf{z} \in C_c$ and moreover $\mathbf{z} \in B_{r_k/2}(\mathbf{z}_k)$ for some $k \in \{1, \dots, K\}$. Thus, the triangle inequality implies $\mathbf{x}_L \in B_{r_k}(\mathbf{z}_k)$ and therefore we conclude $\mathbf{x}_L, \mathbf{x}_{L+1}, \dots, \mathbf{x}_{L+N}$ is in $U(\mathbf{z}_k)$. Since \mathbf{x}_{L+N} again satisfies $d(\mathbf{x}_{L+N}, C_c) < r_*$ we can repeat the above arguments and obtain $\mathbf{x}_{L+N}, \mathbf{x}_{L+N+1}, \dots, \mathbf{x}_{L+2N}$ are in some $U(\mathbf{z}_{k'})$, etc. Combining this observation with Cor. 3.13 we get

$$\Pr(\mathbf{x}_i \rightarrow C_c \text{ for } i \rightarrow \infty) \leq \sum_{L=1}^{\infty} \Pr_L = 0,$$

where \Pr_L is defined by

$$\Pr_L := \Pr \left(\forall i \geq L : f(\mathbf{x}_i) \geq c \wedge \forall m \in \mathbb{N} \exists k \in \{1, \dots, K\} : \mathbf{x}_{L+(m-1)N}, \dots, \mathbf{x}_{L+mN} \in U(\mathbf{z}_k) \right) = 0.$$

Above we used the fact that by Markovianity the behavior of each sequence of N consecutive steps behaves independently. Since there are only finitely many critical submanifolds contained in C it follows that there are only finitely many $c \leq f(\mathbf{x}_0)$ such that $C_c \neq \emptyset$ and thus we conclude that the probability that \mathbf{x}_i converges to C is also zero. \square

3.3 Almost Sure Convergence

The results proven so far guarantee that the algorithm (cp. Fig. 1) converges almost surely to the set of local minima:

Proposition 3.15. *Let M be a Riemannian manifold and let $f : M \rightarrow \mathbb{R}$ be an ℓ -smooth Morse–Bott function with compact sublevel sets. Assume that \mathbf{x}_0 is not a critical point. Then, for stepsize $\eta \leq 1/\ell$, the randomized gradient descent algorithm converges almost surely to the set of local minima.*

Proof. Since by Lem. 3.7 the function value cannot increase, and since by compactness of sublevel sets the function is lower bounded, the function value must (surely) converge to some value f^* . By Cor. 3.8, f^* is almost surely a critical value. By Lem. 3.14 the algorithm almost surely does not converge towards the set of strict saddle points. Hence it has converge almost surely to the set of local minima. \square

In order to prove convergence to a single local minimum, we first need the following technical lemma.

Lemma 3.16. *Let \mathcal{E}_i be probability distributions over the interval $[0, 1]$ and let $E_i \sim \mathcal{E}_i$ for $i \in \mathbb{N}$. Let $\varepsilon > 0$ be given. We assume that there is $q > 0$ such that*

$$\Pr(E_i \geq \varepsilon \mid E_1, \dots, E_{i-1}) \geq q$$

for all $i \in \mathbb{N}$. Then for any $\alpha \in (0, q \ln \frac{1}{1-\varepsilon})$ it holds that almost surely

$$\prod_{i=1}^n (1 - E_i) \leq e^{-\alpha n}$$

for n large enough.

Proof. First recall the following basic fact. Consider a sequence of i.i.d. biased coin tosses $X_i \in \{0, 1\}$ with $\Pr(X_i = 1) = q$. By the strong law of large numbers (Jacod and Protter, 2004, Thm. 20.1) the average $\bar{X}_n = \frac{1}{n} \sum_{i=1}^n X_i$ converges almost surely to the expectation q . Hence for any $p \in (0, q)$, there almost surely exists some n_0 large enough such that $\bar{X}_n \geq p$ for all $n > n_0$.

Let any value n , and index set $I = \{i_1, \dots, i_k\} \subseteq \{1, \dots, n\}$ (ordered increasingly) be given. Then, using the law of total probability,

$$\begin{aligned} \Pr(E_i \geq \varepsilon, \forall i \in I) &= \Pr(E_{i_k} \geq \varepsilon \wedge \dots \wedge E_{i_1} \geq \varepsilon) \\ &= \Pr(E_{i_k} \geq \varepsilon \mid E_{i_{k-1}} \geq \varepsilon \wedge \dots \wedge E_{i_1} \geq \varepsilon) \dots \Pr(E_{i_1} \geq \varepsilon) \\ &\geq q^k \\ &= \Pr(X_{i_k} = 1, \dots, X_{i_1} = 1) \end{aligned}$$

and thus we have the following: For all $p \in (0, q)$, there almost surely exists some n_0 large enough such that for all $n > n_0$ it holds that at least pn of the E_i are greater

than or equal to ε . In this case

$$\prod_{i=1}^n (1 - E_i) \leq (1 - \varepsilon)^{np} = e^{-\alpha n},$$

with $\alpha = p \ln \frac{1}{1-\varepsilon}$. □

Finally this allows us to prove the main result:

Theorem 3.17. *Let M be a Riemannian manifold and let $f : M \rightarrow \mathbb{R}$ be an ℓ -smooth Morse–Bott function with compact sublevel sets. Further assume that \mathbf{x}_0 is not a critical point of f . Then, for step size $\eta \leq 1/\ell$, the randomly projected gradient descent algorithm converges almost surely to a local minimum.*

Proof. The idea of the proof is as follows: first we show that almost surely the distance to the set of local minima decreases exponentially. Then this implies that the size of each step decreases exponentially as well, and hence the algorithm converges absolutely to a local minimum.

Prop. 3.15 shows that \mathbf{x}_i converges almost surely to some set of local minima denoted C . Let $\mathbf{z} \in C$ be such a local minimum, and let $H(\mathbf{z})$ denote the Hessian at \mathbf{z} , and let $a_{\min}(\mathbf{z})$ denote the smallest non-zero eigenvalue of $H(\mathbf{z})$. Assume w.l.o.g. that $f(\mathbf{z}) = 0$. By compactness and continuity $a_{\min}(\mathbf{z})$ has a minimum on C , which we denote a_{\min} . In a sufficiently small neighborhood of \mathbf{z} , working in a chart as provided by Lem. 3.12, we obtain

$$\begin{aligned} \|\text{grad } f(\mathbf{x})\|^2 &= \sum_j 4a_j(\mathbf{z})^2 (x_j - z_j)^2 + \mathcal{O}(\|\mathbf{x} - \mathbf{z}\|^3) \\ &\geq 4a_{\min}(\mathbf{z})f(\mathbf{x}) + \mathcal{O}(\|\mathbf{x} - \mathbf{z}\|^3) \\ &\geq 2a_{\min}(\mathbf{z})f(\mathbf{x}). \end{aligned}$$

Together with Lem. 3.7 and Cor. 3.4 we find

$$f(\mathbf{x}_{i+1}) \leq \left(1 - ((\mathbf{u}_i)_N)^2 \delta 2a_{\min}\right) f(\mathbf{x}_i)$$

with $\delta = \eta(1 - \frac{\ell\eta}{2}) < \frac{1}{2a_{\min}}$. By Lem. 3.16, applied to $E_i = ((\mathbf{u}_i)_N)^2 \delta 2a_{\min}$, this shows that there is some $\alpha > 0$ such that $f(\mathbf{x}_i) \leq f(\mathbf{x}_0)e^{-\alpha i}$ almost surely for i large enough. Again by Lem. 3.7 we have that

$$\|\mathbf{x}_{i+1} - \mathbf{x}_i\| \leq \sqrt{\frac{|f(\mathbf{x}_{i+1}) - f(\mathbf{x}_i)|}{\frac{1}{\eta} - \frac{\ell}{2}}}.$$

This shows that for $L \in \mathbb{N}$ large enough we can assume that all \mathbf{x}_i with $i \geq L$ are contained in a single chart of the same kind as in Lem. 3.7 and thus we conclude

$$\sum_{i=L}^{\infty} \|\mathbf{x}_{i+1} - \mathbf{x}_i\| \leq \frac{1}{\sqrt{\frac{1}{\eta} - \frac{\ell}{2}}} \sum_{i=L}^{\infty} \sqrt{f(\mathbf{x}_i)} \leq \sqrt{\frac{f(\mathbf{x}_0)}{\frac{1}{\eta} - \frac{\ell}{2}}} \frac{e^{L\alpha/2}}{1 - e^{\alpha/2}} < \infty,$$

and so the total length of the trajectory is finite. Thus \mathbf{x}_i almost surely converges to a local minimum of f . \square

4 Quantitative Results in Low Dimensions

The goal of this section is to study how long it takes to pass a saddle point. More precisely, we want to understand the hitting time τ of the sublevel set of the critical value at a saddle point. By construction, the discrete stochastic process \mathbf{x}_i is a Markov chain, since the step $\mathbf{x}_{i+1} - \mathbf{x}_i$ depends only on the value of \mathbf{x}_i , and not on previous steps. As such, for small enough step size η , we can approximate the algorithm by an appropriate Ito stochastic differential equation (SDE). As we will see, the accuracy of this approximation improves with smaller step size η , at the cost of slower convergence.

4.1 Two-Dimensional Euclidean Case

In the simplest case, we consider the prototypical Morse function $f(x, y) = x^2 - y^2$ on \mathbb{R}^2 in the Euclidean metric. Due to the scale invariance, we can normalize the state after each iteration and so we obtain a discrete-time stochastic process on the unit circle parametrized by the angle ϕ . For small enough step size $0 < \eta \ll 1$ the iteration rule is approximately¹¹ given by

$$\Delta\phi_i = \phi_{i+1} - \phi_i \stackrel{d}{=} \eta (\sin(2\phi_i) + u_2), \quad (9)$$

where $\mathbf{u} = (u_1, u_2)$ is chosen uniformly at random from the unit circle and hence using Lem. A.1 we find that

$$\mathbb{E}[\Delta\phi_i] = \eta \sin(2\phi_i), \quad \text{Var}(\Delta\phi_i) = \frac{\eta}{2}.$$

Using (Kloeden and Platen, 1992, Sec. 6.2) we can approximate this process using the stochastic differential equation (SDE)

$$d\Phi_t = \sin(2\Phi_t)dt + \frac{\sqrt{\eta}}{2}dW_t, \quad (10)$$

where W_t denotes a standard Brownian motion. The approximation is visualized in Fig. 2.

¹¹The formula is obtained by locally approximating the unit circle by its tangent line. More precisely, we define $\Delta\phi = -\eta \langle \mathbf{u}, \nabla f \rangle \langle \mathbf{u}, \mathbf{v} \rangle$ where $\mathbf{v} = (-\sin \phi, \cos \phi)$. Then $\Delta\phi = \eta \sin(2\phi) - \eta 2u_1 u_2 \stackrel{d}{=} \eta \sin(2\phi) + \eta u_2$.

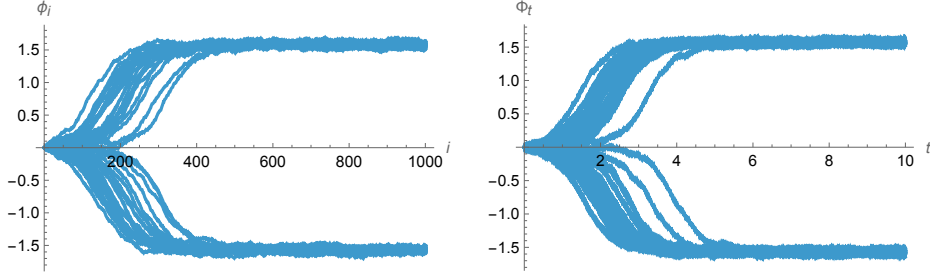


Fig. 2 We use the step size $\eta = 0.01$, total time $T = 10$, and initial state $\phi_0 = \Phi_0 = 0$. Left: 50 realizations of the discrete-time stochastic process (9) for $T/\eta = 1000$ steps. Right: 50 realizations of the continuous-time stochastic process (10) for time $T = 10$, simulated using the Euler–Maruyama scheme (Kloeden and Platen, 1992, Sec. 9.1) with time step size $\Delta t = 0.001$.

In order to understand how long it takes the algorithm to pass the saddle point, we are interested in computing the hitting time

$$\tau = \inf\{t \geq 0 : \Phi_t = \pm \frac{\pi}{4}\},$$

where we always assume that $\Phi_0 = 0$. Close to 0, the SDE can be linearized as $d\Phi_t = 2\Phi_t dt + \frac{\sqrt{\eta}}{2} dW_t$, which is a mean-repelling Ornstein–Uhlenbeck process. Away from 0, the deterministic part dominates and we can solve the (deterministic) ODE $\dot{\Phi}_t = \sin(2\Phi_t)$.

First we approximate the hitting time distribution of the mean-repelling Ornstein–Uhlenbeck process. More precisely, we find a lower bound on the cumulative distribution function (c.d.f.) of τ_c , the hitting time of $\pm c$.

Lemma 4.1. *Let X_t be the solution of the SDE $dX_t = \kappa X_t dt + \sigma dW_t$ with $\kappa, \sigma > 0$ and $X_0 = 0$. Setting $\tilde{\sigma}(t) = \sigma \sqrt{\frac{e^{2\kappa t} - 1}{2\kappa}}$, it holds that $X_t \sim \mathcal{N}(0, \tilde{\sigma}(t)^2)$. If we denote by τ_c the hitting time of $\pm c$ (where $c > 0$), we find the lower bound $\Pr[\tau_c \leq t] \geq \Pr[|X_t| \geq c] = 1 + \operatorname{erf}\left(\frac{-c}{\tilde{\sigma}(t)\sqrt{2}}\right)$ where $\operatorname{erf}(\cdot)$ denotes the error function.*

Proof. The SDE is linear and hence has the well-known solution

$$X_t = \sigma \int_0^t e^{\kappa(s-t)} dW_s \sim \mathcal{N}(0, \tilde{\sigma}(t)^2),$$

where $\tilde{\sigma}(t) = \sigma \sqrt{\frac{e^{2\kappa t} - 1}{2\kappa}}$, see (Kloeden and Platen, 1992, Sec. 4.2 & 4.4). It is clear that if $|X_t| \geq c$ then $\tau_c \leq t$, which implies the last statement. \square

The approximation is very accurate, as illustrated in Fig. 3. The following remark gives some details on the quality of the approximation.

Remark 4.2. *As in the proof of Lem. 4.1 the solution of the SDE with initial condition $X_0 = c$ is given by*

$$X_t = e^{\kappa t} c + \sigma \int_0^t e^{\kappa(s-t)} dW_s.$$

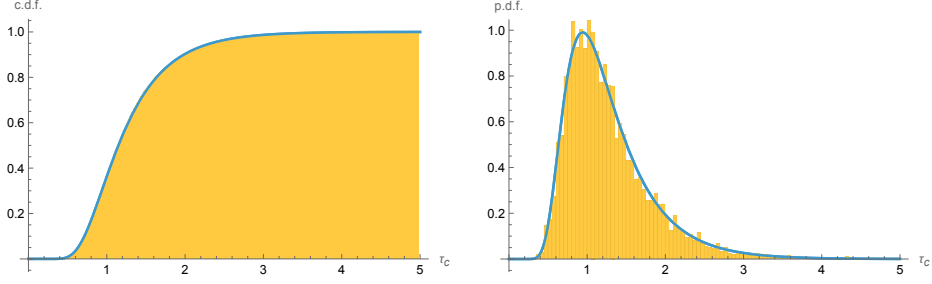


Fig. 3 Lower bound for the hitting time τ_c of the mean-repelling Ornstein–Uhlenbeck process, as obtained in Lem. 4.1. We used the constants $\kappa = 2$, $\sigma = 3$ and $c = 10$. Shown are the histograms of the cumulative distribution function (c.d.f.) and probability density function (p.d.f.) of τ_c for the SDE $dX_t = \kappa X_t dt + \sigma dW_t$ computed using time steps of size 0.001 (orange), and the analytical lower bound for the c.d.f. and the resulting p.d.f. obtained in Lem. 4.1 (blue).

Then

$$e^{\kappa t} c - n\tilde{\sigma}(t) \geq c \implies c \geq n\sigma \sqrt{\frac{e^{2\kappa t} - 1}{2\kappa}} \frac{1}{e^{\kappa t} - 1} \geq \frac{n\sigma}{\sqrt{2\kappa}} \max\left(1, \sqrt{\frac{2}{\kappa t}}\right).$$

Hence, for the error in τ_c to be small compared to some given $t > 0$, we need $c \gg \frac{\sigma}{\sqrt{\kappa}}$ if κt is big, and $c \gg \frac{\sigma}{\kappa\sqrt{t}}$ if κt is small.

Now if we choose c small enough that the linearization of $\sin(\cdot)$ is accurate, but large enough that the approximation of Lem. 4.1 is good (which is always possible if η is small enough), then we can approximate τ as follows.

We fix some value c and note that the ODE $\dot{\phi}(t) = \sin(2\phi(t))$ with initial condition $\phi(0) = c$ has the solution $\phi(t) = \arctan(e^{2t} \tan(c))$, and hence the hitting time of $\pi/4$ is $\tilde{\tau}_c = -\frac{1}{2} \ln(\tan(c))$. Hence we have approximately $\tau \simeq \tau_c + \tilde{\tau}_c$. This is illustrated in Fig. 4 for realistic values.

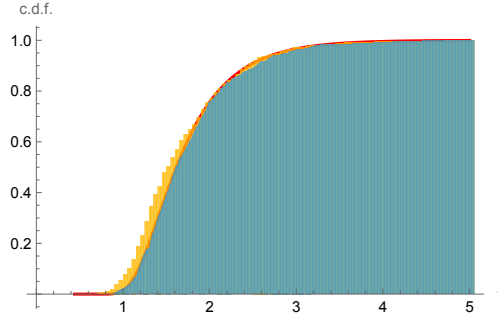


Fig. 4 Using $\eta = 0.05$ we plot the c.d.f. of the hitting time τ of $\frac{\pi}{4}$. In orange for the difference equation (9), in blue for the stochastic differential equation (10) (with time step $\Delta t = 0.001$), and in red for the analytic approximation as described above.

5 Major Application: Ground-State Optimization in Quantum Physics

Among the Riemannian optimization techniques adopted in quantum information science, hybrid quantum-classical algorithms [Bharti et al \(2022\)](#) such as variational quantum algorithms (VQAs) [Cerezo et al \(2021\)](#); [Tilly et al \(2022\)](#), have been developed to solve ground-state (smallest eigenvalue) problems [Peruzzo et al \(2014\)](#).

From the perspective of quantum information and computation, in VQAs, a fixed parameterized quantum circuit, i.e. a parameterized set of unitary transformations (usually implemented by a fixed set of unitary gates), is iteratively optimized in tandem with a classical computer to minimize a cost function whose global optima encode the solution(s) to the desired problem. More precisely, a quantum computer, including a measurement device, is used to output the current (e.g., expectation) value of the cost function in each iterative step. Interleaved, a classical computer component provides the optimization routine that determines the parameter update for the next iteration on the quantum computer. Since quantum computers can, in principle, handle some classically exponentially complex problems, the hope is that VQAs will be able to solve problems of large size that a solely classical algorithm would be incapable of.

However, since the optimization problems VQAs aim to solve are highly non-linear, which can often be traced back to the quantum circuit parametrization [Magann et al \(2021\)](#); [Lee et al \(2021\)](#), the iterative search for the optimal parameters can get stuck in suboptimal solutions [Bittel and Kliesch \(2021\)](#). To overcome this challenge, adaptive quantum algorithms have been designed. Instead of fixing a quantum circuit and picking a parametrization as in VQAs, adaptive algorithms successively grow a quantum circuit based on measurement data from the quantum computer. In this approach, the cost function is minimized *while* the quantum circuit is grown, see [Grimsley et al \(2019\)](#); [Wiersema and Killoran \(2023\)](#); [Magann et al \(2022, 2023\)](#). One of the most prominent examples of such a strategy is the so-called ADAPT-VQE algorithm [Grimsley et al \(2019\)](#), which was originally proposed to solve ground state problems in chemistry, and was further developed later to solve combinatorial optimization problems on quantum computers [Tang et al \(2021\)](#).

Unfortunately, since typically in adaptive quantum algorithms the circuit growth is informed by gradient estimates performed by the quantum computer, adaptive quantum algorithms face similar challenges as VQAs, i.e. the adaptive circuit growth can get stuck when gradients (asymptotically) vanish. This issue has recently been addressed by identifying adaptive quantum algorithms as quantum-computer implementations of Riemannian gradient flows on the special unitary group $SU(d)$ of dimension $d = 2^n$ where n is the number of qubits of the quantum computer [Wiersema and Killoran \(2023\)](#). Since implementing Riemannian gradient methods on quantum computers requires in general exponential resources (i.e. the number of gates or the number of iterations of the corresponding quantum circuit grows exponentially in n), [Wiersema and Killoran \(2023\)](#) proposed projecting the Riemannian gradient into smaller dimensional subspaces that scale polynomially in n , which in turn

yields scalable quantum-computer implementations. As already mentioned, “dimension reduction” for efficient quantum-computer implementations comes at the cost of convergence not only to local minima of the cost function but also to artificial minima induced by projections of the full Riemannian gradient into fixed subspaces. These artifacts can be avoided by “random projections” of the Riemannian gradient [Magann et al \(2023\)](#). The random projections can be implemented on quantum computers as depicted in Figs. 1 and 5. More precisely, an efficient quantum-computer implementation of these random directions can be achieved through exact *and* approximate unitary 2-designs [Dankert et al \(2009\)](#).

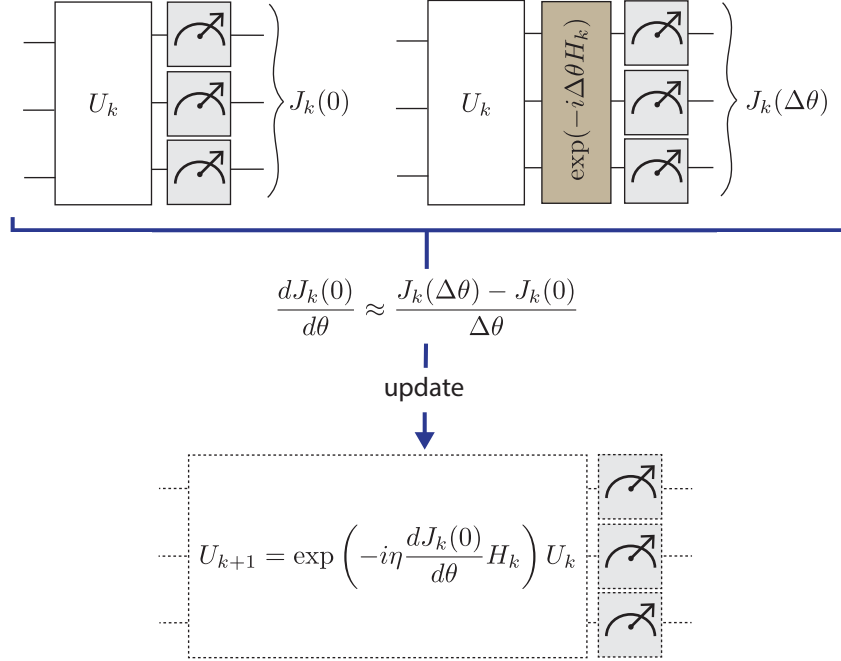


Fig. 5 Schematic implementation of the discretized Riemannian gradient scheme by a quantum algorithm in case the manifold is $M = \text{SU}(2^n)$. Thus the dimension of the problem scales exponentially with the number n of quantum particles (qubits). Each quantum circuit $U_k \in \text{SU}(2^n)$ is adaptively turned into $U_{k+1} = \exp\left(-i\eta \frac{dJ_k(0)}{d\theta} H_k\right) U_k$ by moving in a random tangent-space direction iH_k whose corresponding projection $\frac{dJ_k(0)}{d\theta} = \langle \text{grad} J(U_k), iH_k U_k \rangle$ is measured on a quantum device. Here η denotes the step size and $J_k(\theta)$ the cost function $\theta \mapsto J_k(\theta) := \text{tr}(A \exp(-i\theta H_k) U_k \rho U_k^* \exp(i\theta H_k))$ of the k -th iteration. The measurement of $J_k(\theta)$ is done on the quantum computer, and the statistics of repeated measurements to obtain the expectation value is done on a classical computer. In this way a randomized gradient flow as in Fig. 1 is implemented. In this work we show that for sufficiently small η such a (discretized) flow converges almost surely to the global optimum.

To continue the mathematical perspective of ‘ground state’ optimization, i.e. of finding the smallest eigenvalue (‘ground state energy’) of a Hermitian operator A (Hamiltonian) that describes the energy of the system, we leave the general notation

$f : M \rightarrow \mathbb{R}$ above and specialize to the cost function over the unitary group (or orbit) $J : \text{U}(d) \rightarrow \mathbb{R}$ we aim to minimize. For finding the smallest eigenvalue or, more generally, the smallest expectation value of A with respect to the initial state ρ , the cost function is given by

$$J(U) := \text{tr}(AU\rho U^*) =: \langle A, \text{Ad}_U(\rho) \rangle, \quad (11)$$

where ρ is a density matrix representing the initial state of the system and U is a unitary transformation that describes a quantum circuit (writing U^* for the complex conjugate transpose).

By choosing an appropriate eigenbasis of A , we may assume that A is diagonal with eigenvalues in non-increasing order. The function we want to optimize is of the form of Eqn. (11). Many properties of this function can be found in [Duistermaat et al \(1983\)](#) in the more general setting of semisimple Lie groups. We recall the relevant properties here, adapted to our setting:

Proposition 5.1. *Assume that ρ and A are diagonal¹². Then the following hold.*

- (i) *U is a critical point of f if and only if $[A, \text{Ad}_U(\rho)] = 0$. Hence, the critical set of J is equal to*

$$\text{SU}(d)_A \mathcal{S}_d \text{SU}(d)_\rho,$$

where \mathcal{S}_d is the set of d by d permutation matrices and $\text{SU}(d)_A$, $\text{SU}(d)_\rho$ denote the stabilizer subgroups for the action of conjugation. In particular, it is a disjoint union of finitely many compact connected submanifolds.

- (ii) *The Hessian at a critical point U is determined by*

$$\frac{d^2}{dt^2} \langle A, \text{Ad}_{e^{itH}}(\rho) \rangle = \sum_{i>j} 2(a_i - a_j)(\rho_i - \rho_j) |\langle i | \text{Ad}_U(H) | j \rangle|^2,$$

and in particular J is Morse–Bott.¹³

- (iii) *There is only one local minimal (resp. maximal) value.*

Proof. (i): See Lem. 1.1 and Props. 1.2 and 1.3 of [Duistermaat et al \(1983\)](#). (ii): See Prop. 1.4 and Cor. 1.5 of [Duistermaat et al \(1983\)](#). (iii): See Rmk. 1.6 of [Duistermaat et al \(1983\)](#). \square

A key tool for the experimental implementation of the randomized gradient descent algorithm on quantum hardware are unitary t -designs, whose purpose is to efficiently implement random unitaries.

Definition 5.2 (Thm. 3 in [Gross et al \(2007\)](#)). *A unitary representation $\pi : G \rightarrow \text{U}(d)$, $g \mapsto \pi(g) =: U_g$ of a finite group G is called a unitary t -design with $t \in \mathbb{N}_0$ if one of the following equivalent conditions is satisfied:*

¹²This amounts to a shift in the function J which results from an appropriate choice of $U := U_0^* V_0$ and the identity $\text{tr}(A(U_0^* V_0) \rho (U_0^* V_0)^*) = \text{tr}(U_0 A U_0^* V_0 \rho V_0^*)$.

¹³Note that the function J is never Morse, since the maximal torus in $\text{SU}(d)$ stabilizes A and ρ .

(a) For all polynomials $p \in \mathbb{C}_t[Z, \bar{Z}]$ one has the equality

$$\frac{1}{|G|} \sum_{g \in G} p(U_g, \bar{U}_g) = \int_{U(d)} p(U, \bar{U}) dU,$$

where $\mathbb{C}_t[Z, \bar{Z}]$ denotes the set of all polynomials in $Z := (z_{ij})_{i,j=1,\dots,d}$ and $\bar{Z} := (\bar{z}_{ij})_{i,j=1,\dots,d}$, which are t homogeneous in Z and \bar{Z} , i.e.¹⁴ with $p(\lambda Z, \mu \bar{Z}) = \lambda^t \mu^t p(Z, \bar{Z})$.

(b) For all $H \in \mathbb{C}^{d^t \times d^t}$ one has the equality

$$\frac{1}{|G|} \sum_{g \in G} (U_g \otimes \dots \otimes U_g) H (U_g \otimes \dots \otimes U_g)^* = \int_{U(d)} (U \otimes \dots \otimes U) H (U \otimes \dots \otimes U)^* dU.$$

(c) One has the equality

$$\frac{1}{|G|} \sum_{g \in G} (U_g \otimes \dots \otimes U_g) \otimes (\bar{U}_g \otimes \dots \otimes \bar{U}_g) = \int_{U(d)} (U \otimes \dots \otimes U) \otimes (\bar{U} \otimes \dots \otimes \bar{U}) dU.$$

For $t = 2$ one has the further equivalence

(d) The tensor square representation $\pi \otimes \pi : G \rightarrow U(d) \otimes U(d)$, $g \mapsto U_g \otimes U_g$ acting on $\mathbb{C}^d \otimes \mathbb{C}^d$ has exactly two irreducible components, namely $\text{Sym}(\mathbb{C}^d \otimes \mathbb{C}^d)$ and $\text{Alt}(\mathbb{C}^d \otimes \mathbb{C}^d) := \mathbb{C}^d \wedge \mathbb{C}^d$.

Remark 5.3. A more general notion of t -designs [Dankert \(2006\)](#); [Dankert et al \(2009\)](#) (see also [Gross et al \(2007\)](#)) allows any finite subset of $U(d)$ which satisfies (a), (b) or, equivalently, (c). However, since almost all known examples are constructed via group representations, we focus here on this restricted approach which is sometimes called group design. Moreover, the reader should note the following facts: (i) One can assume without loss of generality that π is faithful (i.e., one-to-one) because it is straightforward to show that $[g] \mapsto \pi(g)$, $[g] \in G/\ker \pi$ yields a t -design whenever π is a t -design. (ii) Every t -design is also t' -design for $t' \leq t$. This follows readily from condition (b) by choosing H of the form $H' \otimes I_n \otimes \dots \otimes I_n$.

Now we need the following technical lemma:

Lemma 5.4. Let $\pi : G \rightarrow U(d)$ be any unitary representation. Then π yields a 2-design in the sense of Def. 5.2 if and only if π acts irreducibly on $\mathfrak{su}(n)$ via conjugation, i.e. the representation $\hat{\pi} : G \rightarrow U(\mathfrak{su}(d))$, $\pi(g) H := U_g H U_g^*$ is irreducible.

Proof. First, $\hat{\pi}$ obviously “extends” to $\tilde{\pi} : G \rightarrow U(\mathbb{C}^{d \times d})$, $\tilde{\pi}(g) A := U_g A U_g^{-1}$. Then a straightforward computation shows that the representations $\tilde{\pi}$ and $g \mapsto U_g \otimes \bar{U}_g$ are equivalent and thus for simplicity we will use the same symbol for both representations.

¹⁴This is equivalent to $p(\lambda Z, \bar{\lambda} \bar{Z}) = |\lambda|^{2t} p(Z, \bar{Z})$.

Next, we investigate the commutant of the representations $U_g \otimes \bar{U}_g$ and $U_g \otimes U_g$ in $\mathbb{C}^{d \times d} \otimes \mathbb{C}^{d \times d} \cong \mathbb{C}^{d^2 \times d^2}$, i.e. we are interested in the solutions Z of

$$(U_g \otimes \bar{U}_g)Z = Z(U_g \otimes \bar{U}_g) \quad \text{for all } g \in G, \quad (12)$$

and

$$(U_g \otimes U_g)Z = Z(U_g \otimes U_g) \quad \text{for all } g \in G, \quad (13)$$

respectively. Eq. (12) and (13) are equivalent to $\text{Ad}_{U_g \otimes \bar{U}_g}(Z) = Z$ and $\text{Ad}_{U_g \otimes U_g}(Z) = Z$, respectively. Finally, a tedious but straightforward computation shows that the partial transposed operator $\Phi : \mathbb{C}^{d \times d} \otimes \mathbb{C}^{d \times d} \rightarrow \mathbb{C}^{d \times d} \otimes \mathbb{C}^{d \times d}$, $A \otimes B \mapsto A \otimes B^T$ yield an intertwining map for $\text{Ad}_{U_g \otimes \bar{U}_g}$ and $\text{Ad}_{U_g \otimes U_g}$, i.e.

$$\text{Ad}_{U_g \otimes \bar{U}_g} \circ \Phi = \Phi \circ \text{Ad}_{U_g \otimes U_g}.$$

This implies Φ maps the commutator of $\tilde{\pi}$ to the commutator of $\pi \otimes \pi$ and therefore the dimensions of commutators (and consequently the number of irreducible subspaces) coincide. Thus $\text{Sym}(\mathbb{C}^d \otimes \mathbb{C}^d)$ and $\text{Alt}(\mathbb{C}^d \otimes \mathbb{C}^d)$ are the only irreducible subspaces of $\pi \otimes \pi$ if and only if $\mathbb{C}I_d$ and $\mathfrak{sl}_0(d)$ are the only irreducible subspaces to $\tilde{\pi}$ (or, equivalently, $\mathfrak{isu}(d)$ is the only irreducible subspace of $\hat{\pi}$). \square

Remark 5.5. Note that the above result does not mean that the tensor square representation $\pi \otimes \pi$ and $\tilde{\pi}$ are equivalent and, in fact, they are not — as easy examples demonstrate. A similar result for Lie algebra representations was elaborated on in Zeier and Zimborás (2015) as follow-up to Zeier and Schulte-Herbrüggen (2011) and in particular to Coquereaux and Zuber (2011).

The following is the main result of this section, showing that unitary 2-designs satisfy Assumption 3.1. As a consequence, the main convergence result (Thm. 3.17) applies to the problem considered in this section.

Proposition 5.6. Let $\pi : G \rightarrow \text{U}(n)$ be a unitary t -design with $t \geq 2$ and let $H_s \in \mathfrak{isu}(n)$ be a traceless Hermitian matrix. Then any subset of $\{U_g H_s U_g^* : g \in G\}$, where one element is removed, still spans $\mathfrak{isu}(n)$.

Proof. By Lem. 5.4 we know that the $\hat{\pi}$ -invariant subspace spanned by $\{U_g H_s U_g^* : g \in G\}$ has to coincide with $\mathfrak{isu}(d)$ and thus $\{U_g H_s U_g^* : g \in G\}$ contains a basis of $\mathfrak{isu}(d)$. Moreover, by the defining property (b) it is straightforward to see that every 1-design, and therefore also every 2-design, has to act irreducibly on \mathbb{C}^d . Thus we conclude

$$\sum_{g \in G} U_g H_s U_g^* = 0$$

because the left hand side of the above equation belongs to the commutant of π and has trace zero. Now if there is some $g_0 \in G$ such that $\{U_g H_s U_g^* : g \in G, g \neq g_0\}$ does not span $\mathfrak{isu}(d)$, then $U_{g_0} H_s U_{g_0}^*$ does not lie in the span of the others, and hence $\sum_{g \in G} U_g H_s U_g^* \neq 0$, which contradicts the above. \square

Corollary 5.7. *The randomized gradient descent algorithm introduced in Sec. 3, applied to the cost function (11) on the unitary group, with randomly chosen directions $\{U_g H_s U_g^*\}_{g \in G}$ as in Prop. 5.6, converges almost surely to a global minimum. Moreover, by continuity, this continues to hold if U_g is an approximate 2-design, as long as the approximation is good enough.*

On the Orbit

Since the map $J : \text{SU}(d) \rightarrow \mathbb{R}$, which depends on the initial state ρ , is invariant under the stabilizer subgroup of ρ , denoted $\text{SU}(d)_\rho$, the map can be factored through the corresponding quotient space. Equivalently, one may define the map on the unitary orbit of the initial state ρ . We denote this map by $\bar{J} : \text{SU}(d)_\rho \rightarrow \mathbb{R}$. Working with this function has some theoretical advantages, such as the reduced dimension of the state space. Moreover, in many cases the function is even Morse:

Lemma 5.8. *If A is non-degenerate, then the function \bar{J} is Morse.*

Proof. See (Duistermaat et al, 1983, Coro. 3.7, Sec. 4). □

Despite the nice properties of \bar{J} , we do not use this formulation, since it is not clear how to efficiently sample random unitaries yielding directions in the tangent space of the orbit.

6 Conclusion, Discussion, and Outlook

We have analyzed the convergence properties of a recently introduced Haar-randomly projected gradient descent algorithm for cost functions taking the form of a smooth Morse–Bott function (with compact sublevel sets) on a Riemannian manifold. For making it efficient in quantum optimizations, one can approximate the Haar-random projections via unitary 2-designs. For both scenarios we have proven that (i) the respective algorithm *almost surely escapes saddle points* (Lem. 3.14) and (ii) it *almost surely converges to a local minimum* (Thm. 3.17). Moreover, we have studied the time required by the algorithm to pass a saddle point in a simple two-dimensional setting (Sec. 4.1). Note that unlike adiabatic ground-state preparation strategies (that rest on first preparing some desired initial state to find the ground state of some target Hamiltonian), our randomized Riemannian gradient flow algorithm does not require knowledge of the initial state, as the algorithm converges for almost all initial points. Furthermore, as in the quantum setting for ground state problems the critical points just comprise saddles and global extrema, here our result implies almost sure convergence to the *global minimum*.

However, our approach inherits a key problem already arising without projections: the overall speed of convergence to globally optimal solutions may be slow Magann et al (2023), since it depends on the scaling of the magnitude of the (projected) Riemannian gradient. For Riemannian optimizations over the unitary group, the gradient magnitude converges to its expectation value (being zero), while the variance is inversely proportional to the dimension $d = 2^n$ McClean et al (2018). Thus the probability for a gradient magnitude larger than the noise level of a quantum computer

decays exponentially with the number of qubits n . Well known as *barren plateaux problem* in quantum optimization [McClean et al \(2018\)](#), such exponentially flat regions constitute a main challenge to all variational quantum algorithms in high dimensions on quantum computers.

The algorithmic steps analyzed here are entirely modular. In view of future applications, the (approximate) random projections w.r.t. the Haar measure may well be replaced by selections from other problem-adapted measures without sacrificing the convergence properties. In particular, one may wish to select the measures such that the projections of the gradient do not subside in numerical noise prematurely and thus circumvent the notorious barren plateaux problem. Moreover, one may consider random projections into subspaces by techniques of compressed sensing and shadow tomography to better approximate the full gradient flow. Likewise, approximations with tensor-network methods (such as, e.g., [Vanderstraeten et al \(2016, 2019\)](#)) may be envisaged as long as one remains on a Riemannian manifold. More specifically, see [Miao and Barthel \(2023\)](#) for the connection of trotterized MERA tensor networks with Riemannian optimization (extended to quasi-Newton) of VQAs in view of hybrid quantum computing. Another interesting recent application, which may potentially profit from the random methods described here, is Riemannian quantum circuit optimization based on matrix product operators as suggested by [Le et al \(2025\)](#).

Needless to say, the randomized gradient techniques presented here in this paper lend themselves to be taken over to higher-order quasi Newton methods (like L-BFGS) as described in [Schulte-Herbrüggen et al \(2010\)](#) also on quantum computers.

Thus we anticipate that the convergence guaranteed for (randomized) Riemannian gradient flows with respect to Morse–Bott type smooth cost functions will encourage wide application in and beyond quantum optimization.

Acknowledgements

E.M. and T.S.H. are supported by the *Munich Center for Quantum Science and Technology* (MCQST) and the *Munich Quantum Valley* (MQV) with funds from the Agenda Bayern Plus. C.A. acknowledges support from the National Science Foundation (Grant No. 2231328) and Knowledge Enterprise at Arizona State University.

Conflicts of Interest

All authors declare that they have no conflicts of interest.

Appendix

A Some Technical Results

The probability distributions of u_N and u_N^2 are important for understanding the behavior of the algorithm. Fortunately, they can be described quite easily using the beta distribution. Recall that the p.d.f. of the beta distribution with parameters $a, b > 0$ is given by $f(x) = \text{const} \cdot x^{a-1}(1-x)^{b-1}$.

Lemma A.1. *If $\mathbf{u} \sim \mathcal{U}(S^{N-1})$ and u_N is the last coordinate, then*

$$u_N \sim \mathcal{B}_N := 2 \text{Beta}\left(\frac{N-1}{2}, \frac{N-1}{2}\right) - 1, \quad u_N^2 \sim \mathcal{B}_N^2 := \text{Beta}\left(\frac{1}{2}, \frac{N-1}{2}\right),$$

where $\text{Beta}(a, b)$ denotes the beta distribution, and hence

$$\mathbb{E}[u_N^2] = \frac{1}{N}, \quad \text{Var}(u_N^2) = \frac{2(N-1)}{N^2(N+2)}.$$

Proof. Let Z_1, \dots, Z_N be i.i.d. standard normals. Then, a uniformly random unit vector can be obtained by normalizing the vector $(Z_1, \dots, Z_N) \in \mathbb{R}^N$. Considering the last coordinate we see that $u_N \stackrel{d}{=} Z_N / \sqrt{Z_1^2 + \dots + Z_N^2}$. Hence using a well-known relation between the beta and χ^2 (chi-squared) distributions¹⁵ we find

$$u_N^2 \stackrel{d}{=} \frac{Z_N^2}{(Z_1^2 + \dots + Z_{N-1}^2) + Z_N^2} \sim \text{Beta}\left(\frac{1}{2}, \frac{N-1}{2}\right).$$

Since u_N is symmetrically distributed around 0, it is easy to compute its p.d.f. starting from that of u_N^2 , and one obtains the form given above. The expectation and variance of u_N^2 follow easily from the formula for the moments of a beta distributed variable $X \sim \text{Beta}(a, b)$:

$$\mathbb{E}[X^k] = \prod_{r=0}^{k-1} \frac{a+r}{a+b+r}.$$

This concludes the proof. □

Lemma A.2. *For $N \geq 5$ it holds that*

$$d_K(\sqrt{N}\mathcal{B}_N, \mathcal{N}(0, 1)) \leq \frac{1}{N},$$

where d_K denotes the Kolmogorov distance (the supremum distance between the cumulative distribution functions). This shows that u_N^2 is almost distributed according to the distribution $1/N\chi_1^2$, more precisely

$$d_K(N(\mathcal{B}_N)^2, \chi_1^2) \leq \frac{2}{N}.$$

If Φ denotes the cumulative distribution function of a standard normal distribution, then for any $k \geq 0$ it holds that

$$\Pr\left(u_N^2 \geq \frac{1}{k^2 N}\right) \geq 2\left(1 - \Phi\left(\frac{1}{k}\right) - \frac{1}{N}\right).$$

¹⁵If $X \sim \chi_a^2$ and $Y \sim \chi_b^2$ are independent, then $\frac{X}{X+Y} \sim \text{Beta}\left(\frac{a}{2}, \frac{b}{2}\right)$, see (Balakrishnan and Nevzorov, 2003, Sec. 20.8 and 24.4).

Proof. The first inequality follows from (Pinelis and Molzon, 2016, p. 20) and (Pinelis, 2015, Thm. 1.2). It is easy to see that taking the square of both distributions at most doubles the Kolmogorov distance, and this yields the second inequality. Finally we compute

$$\Pr(u_N^2 \geq \frac{1}{k^2 N}) = 2(1 - \Pr(u_N \leq \frac{1}{k\sqrt{N}})) \geq 2(1 - \Phi(\frac{1}{k}) - \frac{1}{N}),$$

proving the third inequality. \square

References

- Absil PA, Mahony R, Sepulchre R (2008) Optimization Algorithms on Matrix Manifolds. Princeton University Press, Princeton
- Ambrosio L, Brué E, Semola D, et al (2021) Lectures on Optimal Transport, vol 130. Springer
- Audin M (2014) Morse Theory and Floer Homology. Springer, London
- Aulbach B (1984) Continuous and Discrete Dynamics near Manifolds of Equilibria, Lecture Notes in Mathematics LNM, vol 1058. Springer, Berlin, Heidelberg, <https://doi.org/10.1007/BFb0071569>
- Balakrishnan N, Nevzorov V (2003) A Primer on Statistical Distributions. Wiley & Sons, New Jersey
- Banyaga A, Hurtubise D (2004) A Proof of the Morse-Bott Lemma. Expp Math 22:365–373
- Banyaga A, Hurtubise D (2010) Morse-Bott Homology. Trans Am Math Soc 362:3997–4043
- Batselier K, Yu W, Daniel L, et al (2018) Computing Low-Rank Approximations of Large-Scale Matrices with the Tensor Network Randomized SVD. SIAM J Matrix Anal Appl 39:1221–1244
- Berger M (2003) A Panoramic View of Riemannian Geometry. Springer, Berlin Heidelberg
- Bharti K, Cervera-Lierta A, Kyaw TH, et al (2022) Noisy Intermediate-Scale Quantum Algorithms. Rev Mod Phys 94:015004
- Biamonte J, Wittek P, Pancotti N, et al (2017) Quantum Machine Learning. Nature 549(7671):195–202
- Bittel L, Kliesch M (2021) Training Variational Quantum Algorithms Is NP-Hard. Phys Rev Lett 127:120502

- Bloch A (ed) (1994) Hamiltonian and Gradient Flows, Algorithms and Control. Fields Institute Communications, American Mathematical Society, Providence
- Boumal N (2023) An Introduction to Optimization on Smooth Manifolds. Cambridge University Press, Cambridge, <https://doi.org/https://doi.org/10.1017/9781009166164>
- Brockett R (1988) Dynamical Systems That Sort Lists, Diagonalise Matrices, and Solve Linear Programming Problems. In: Proc. IEEE Decision Control, 1988, Austin, Texas, pp 779–803, reproduced in: Lin. Alg. Appl., 146 (1991), 79–91
- Brockett R (1989) Least-Squares Matching Problems. Lin Alg Appl 122-4:761–777
- Brockett R (1993) Differential Geometry and the Design of Gradient Algorithms. Proc Symp Pure Math 54:69–91
- Cerezo M, Arrasmith A, Babbush R, et al (2021) Variational Quantum Algorithms. Nature Rev Phys 3:625–644
- Chu MT, Driessel KR (1990) The Projected Gradient Method for Least-Squares Matrix Approximations with Spectral Constraints. SIAM J Numer Anal 27:1050–1060
- Coquereaux R, Zuber J (2011) On Sums of Tensor and Fusion Multiplicities. J Phys A 44:295208
- Criscitiello C, Boumal N (2019) Efficiently escaping saddle points on manifolds. In: Proceedings of the 33rd International Conference on Neural Information Processing Systems. Curran Associates Inc., Red Hook, NY, pp 5987–5997
- Curry HB (1944) The Method of Steepest Descent for Non-linear Minimization Problems. Q Appl Math 2:258–261
- Curtef O, Dirr G, Helmke U (2012) Riemannian Optimization on Tensor Products of Grassmann Manifolds: Applications to Generalized Rayleigh-Quotients. SIAM J Matrix Anal Appl 33:210 – 234. <https://doi.org/https://doi.org/10.1137/100792032>
- Dankert C (2006) Efficient Simulation of Random Quantum States and Operators, URL <https://doi.org/10.48550/arXiv.quant-ph/0512217>, MSc Thesis Univ. Waterloo
- Dankert C, Cleve R, Emerson J, et al (2009) Exact and Approximate Unitary 2-Designs and Their Application to Fidelity Estimation. Phys Rev A 80:012304
- Duistermaat JJ, Kolk JAC, Varadarajan VS (1983) Functions, Flows and Oscillatory Integrals on Flag Manifolds and Conjugacy Classes in Real Semisimple Lie Groups. Compositio Math 49:309–398

- Farhi E, Goldstone J, Gutmann S (2014) A Quantum Approximate Optimization Algorithm, URL <https://doi.org/10.48550/arXiv.1411.4028>
- Fetecau R, Patacchini F (2022) Well-Posedness of an Interaction Model in Riemannian Manifolds. *Commun Pure Appl Anal* 21:3559–3585
- Grimsley HR, Economou SE, Barnes E, et al (2019) An Adaptive Variational Algorithm for Exact Molecular Simulations on a Quantum Computer. *Nature Comm* 10:3007
- Gross D, Audenaert K, Eisert J (2007) Evenly Distributed Unitaries: On the Structure of Unitary Designs. *J Math Phys* 48:052104
- Gustafson K, Rao D (1997) Numerical Range: The Field of Values of Linear Operators and Matrices. Springer, New York
- Gutman DH, Ho-Nguyen N (2023) Coordinate Descent Without Coordinates: Tangent Subspace Descent on Riemannian Manifolds. *Mathematics of Operations Research* 48(1):127–159. <https://doi.org/10.1287/moor.2022.1253>
- Helmke U, Moore J (1994) Optimisation and Dynamical Systems. Springer, Berlin
- Irwin MC (1980) Smooth Dynamical Systems. Academic Press, New York
- Jacod J, Protter P (2004) Probability Essentials, 2nd edn. Springer, Berlin Heidelberg
- Jin C, Netrapalli P, Ge R, et al (2021) On Nonconvex Optimization for Machine Learning: Gradients, Stochasticity, and Saddle Points. *J ACM* 68(2):1–29
- Kehrein S (2006) The Flow-Equation Approach to Many-Particle Systems, Springer Tracts in Physics, vol 217. Springer, Berlin
- Kloeden PE, Platen E (1992) Numerical Solution of Stochastic Differential Equations. Stochastic Modelling and Applied Probability, Springer, Heidelberg
- Lageman C (2007) Convergence of Gradient-Like Dynamical Systems and Optimization Algorithms. PhD Thesis, Universität Würzburg
- de Lathauwer L, de Moor B, Vandewalle J (2000) On the Best Rank-1 and Rank- (R_1, R_2, \dots, R_n) Approximation of Higher-Order Tensors. *SIAM J Matrix Anal Appl* 21:1324–1342
- Le INM, Sun S, Mendl C (2025) Riemannian Quantum Circuit Optimization Based on Matrix Product Operators, e-print: <http://arXiv.org/pdf/2501.08872>
- Lee J (2013) Introduction to Smooth Manifolds, 2nd edn. Springer, New York

- Lee J, Magann AB, Rabitz HA, et al (2021) Progress toward Favorable Landscapes in Quantum Combinatorial Optimization. *Phys Rev A* 104:032401
- Lee JD, Panageas I, Piliouras G, et al (2019) First-Order Methods Almost Always Avoid Strict Saddle Points. *Math Program* 176:311–337
- Li CK (1994) C -Numerical Ranges and C -Numerical Radii. *Lin Multilin Alg* 37:51–82
- Lojasiewicz S (1984) Sur les Trajectoires du Gradient d’une Fonction Analytique. *Seminari di Geometria 1982-1983*. Università di Bologna, Istituto di Geometria, Dipartimento di Matematica
- Luenberger DG, Ye Y (2008) *Linear and Nonlinear Programming*, 3rd edn. Springer, Berlin
- Magann AB, Arenz C, Grace MD, et al (2021) From Pulses to Circuits and Back Again: A Quantum Optimal Control Perspective on Variational Quantum Algorithms. *PRX Quantum* 2:010101
- Magann AB, Rudinger KM, Grace MD, et al (2022) Feedback-Based Quantum Optimization. *Phys Rev Lett* 129:250502
- Magann AB, Economou SE, Arenz C (2023) Randomized Adaptive Quantum State Preparation. *Phys Rev Res* 5:033227
- McClean JR, Boixo S, Smelyanskiy VN, et al (2018) Barren Plateaux in Quantum Neural Network Training Landscapes. *Nature Commun* 9:4812
- Miao Q, Barthel T (2023) Quantum-Classical Eigensolver Using Multiscale Entanglement Renormalization. *Phys Rev Res* 5:033141. <https://doi.org/10.1103/PhysRevResearch.5.033141>
- Mielke A (2023) An Introduction to the Analysis of Gradient Systems, URL <https://doi.org/10.48550/arXiv.2306.05026>
- Muller JM, Brunie N, de Dinechin F, et al (2018) *Handbook of Floating-Point Arithmetic*, 2nd edn. Birkhäuser, Cham
- Nesterov Y (2004) *Introductory Lectures on Convex Optimization*. Applied Optimization, Springer, New York
- Neuberger J (2010) *Sobolev Gradients and Differential Equations*. Lecture Notes in Mathematics, Springer, Berlin, <https://doi.org/10.1007/978-3-642-04041-2>
- Nicolaescu L (2011) *An Invitation to Morse Theory*, 2nd edn. Springer, New York
- Peruzzo A, McClean J, Shadbolt P, et al (2014) A Variational Eigenvalue Solver on a Photonic Quantum Processor. *Nature Commun* 5:4213

- Pinelis I (2015) Exact Bounds on the Closeness Between the Student and Standard Normal Distributions. *ESAIM: Prob Statistics* 19:24–27
- Pinelis I, Molzon R (2016) Optimal-Order Bounds on the Rate of Convergence to Normality in the Multivariate Delta Method. *Electron J Statist* 10:1001–1063
- Ruder S (2016) An Overview of Gradient Descent Optimization Algorithms, URL <https://doi.org/10.48550/arXiv.1609.04747>
- Savas B, Lim LH (2010) Quasi-Newton Methods on Grassmannians and Multilinear Approximations of Tensors. *SIAM J Scientific Computing* 32:3352 – 3393. <https://doi.org/https://doi.org/10.1137/090763172>
- Schulte-Herbrüggen T, Glaser S, Dirr G, et al (2010) Gradient Flows for Optimisation in Quantum Information and Quantum Dynamics: Foundations and Applications. *Rev Math Phys* 22:597–667
- Smith ST (1993) Geometric Optimization Methods for Adaptive Filtering. PhD Thesis, Harvard University, Cambridge MA
- Smith ST (1994) Hamiltonian and Gradient Flows, Algorithms and Control, American Mathematical Society, Providence, chap Optimization Techniques on Riemannian Manifolds, pp 113–136. Fields Institute Communications
- Sun Y, Flammarion N, Fazel M (2019) Escaping from saddle points on Riemannian manifolds. In: Wallach H, Larochelle H, Beygelzimer A, et al (eds) *Advances in Neural Information Processing Systems*, vol 32. Curran Associates, Inc.
- Takens F (1971) A Solution. In: Kuiper N (ed) *Manifolds - Amsterdam 1970*. Lecture Notes in Math., 197, Springer, New York, p 231
- Tang HL, Shkolnikov V, Barron GS, et al (2021) Qubit-Adapt-VQE: An Adaptive Algorithm for Constructing Hardware-Efficient Ansätze on a Quantum Processor. *PRX Quantum* 2:020310
- Tilly J, Chen H, Cao S, et al (2022) The Variational Quantum Eigensolver: A Review of Methods and Best Practices. *Phys Reports* 986:1–128
- Vanderstraeten L, Haegeman J, Corboz P, et al (2016) Gradient Methods for Variational Optimization of Projected Entangled-Pair States. *Phys Rev B* 94:155123
- Vanderstraeten L, Haegeman J, Verstraete F (2019) Tangent-Space Methods for Uniform Matrix Product States. *SciPost Phys Lect Notes* 7:1–77
- Wegner F (1994) Flow-Equations for Hamiltonians. *Ann Phys (Leipzig)* 3:77–91
- Wiersema R, Killoran N (2023) Optimizing Quantum Circuits with Riemannian Gradient Flow. *Phys Rev A* 107:062421

- Zeier R, Schulte-Herbrüggen T (2011) Symmetry Principles in Quantum System Theory. J Math Phys 52:113510
- Zeier R, Zimborás Z (2015) On Squares of Representations of Compact Lie Algebras. J Math Phys 56:081702